REDUCING MIMO DETECTION COMPLEXITY VIA HIERARCHICAL MODULATION

A THESIS SUBMITTED TO
THE GRADUATE SCHOOL OF NATURAL AND APPLIED SCIENCES
OF
MIDDLE EAST TECHNICAL UNIVERSITY

BY

YİĞİT UĞUR

IN PARTIAL FULFILLMENT OF THE REQUIREMENTS
FOR
THE DEGREE OF MASTER OF SCIENCE
IN
ELECTRICAL AND ELECTRONICS ENGINEERING

AUGUST 2014

Approval of the thesis:

REDUCING MIMO DETECTION COMPLEXITY VIA HIERARCHICAL MODULATION

submitted by **YİĞİT UĞUR** in partial fulfillment of the requirements for the degree of **Master of Science in Electrical and Electronics Engineering Department, Middle East Technical University** by,

Prof. Dr. Canan Özgen
Dean, Graduate School of **Natural and Applied Sciences** _____

Prof. Dr. Gönül Turhan Sayan
Head of Department, **Electrical and Electronics Engineering** _____

Assoc. Prof. Dr. Ali Özgür Yılmaz
Supervisor, **Electrical and Electonics Eng. Dept., METU** _____

Examining Committee Members:

Prof. Dr. Yalçın Tanık
Electrical and Electronics Engineering Department, METU _____

Assoc. Prof. Dr. Ali Özgür Yılmaz
Electrical and Electronics Engineering Department, METU _____

Assoc. Prof. Dr. Melek Diker Yücel
Electrical and Electronics Engineering Department, METU _____

Assoc. Prof. Dr. Çağatay Candan
Electrical and Electronics Engineering Department, METU _____

Dr. Defne Aktaş
Lead Design Engineer, ASELSAN _____

Date: 25.08.2014

I hereby declare that all information in this document has been obtained and presented in accordance with academic rules and ethical conduct. I also declare that, as required by these rules and conduct, I have fully cited and referenced all material and results that are not original to this work.

Name, Last Name: YİĞİT UĞUR

Signature :

ABSTRACT

REDUCING MIMO DETECTION COMPLEXITY VIA HIERARCHICAL MODULATION

Uğur, Yiğit
M.S., Department of Electrical and Electronics Engineering
Supervisor : Assoc. Prof. Dr. Ali Özgür Yılmaz

August 2014, 55 pages

This work considers multiple-input multiple-output (MIMO) communication systems using hierarchical modulation. A disadvantage of the maximum-likelihood (ML) MIMO detector is that its computational complexity increases exponentially with the number of transmit antennas. To reduce complexity, we propose a hierarchical modulation scheme to be used in MIMO transmission where base and enhancement layers are incorporated. In the proposed receiver, the base layer is detected first with a minimum mean square error (MMSE) detector which is followed by ML detection of the enhancement layer. Our results indicate that performance close to ML detection can be achieved with the proposed scheme, yet at a significantly lower complexity.

Keywords: Hierarchical modulation, multiple-input multiple-output (MIMO), computational complexity, minimum mean square error (MMSE), maximum-likelihood (ML), successive interference cancellation (SIC), block fading channel, low-density parity-check (LDPC) codes, error rate.

ÖZ

HİYERARŞİK KİPLEME KULLANILARAK ÇOK-GİRDİLİ ÇOK-ÇIKTILI SEZİMDEKİ KARMAŞIKLIĞIN DÜŞÜRÜLMESİ

Uğur, Yiğit
Yüksek Lisans, Elektrik ve Elektronik Mühendisliği Bölümü
Tez Yöneticisi : Doç. Dr. Ali Özgür Yılmaz

Ağustos 2014, 55 sayfa

Bu çalışmada hiyerarşik kiplemenin çok-girdili çok-çıktılı (MIMO) iletişim sistemlerinde kullanımı incelenmektedir. En büyük olabilirlik (ML) alıcısının işlem yükü verici anten sayısıyla üstel bir şekilde artmaktadır. Alıcı karmaşıklığını düşürmek için temel katman ve iyileştirme katmanlarından oluşan hiyerarşik kipleme tekniği kullanılmıştır. Önerilen yapıda ilk olarak temel katman en küçük ortalama kare hata (MMSE) alıcısı ile çözülür, iyileştirme katmanı çözümüne ML sezici ile devam edilir. Sonuçlarımız, çok daha düşük işlem yüküne sahip önerilen alıcı yapısı ile ML alıcının başarımına yaklaşıldığını göstermektedir.

Anahtar Kelimeler: Hiyerarşik kipleme, çok-girdili çok-çıktılı iletişim sistemi, alıcı işlem yükü, en küçük ortalama kare hata, en büyük olabilirlik, ardışık girişim iptali, blok sönümlemeli kanal, düşük yoğunluklu eşlik denetim kodları, hata oranı.

to my family

ACKNOWLEDGMENTS

First and foremost, I would love to express my sincere gratitude to my advisor Assoc. Prof. Dr. Ali Özgür Yılmaz. His guidance, knowledge and support was the main factor that I am able to finish my thesis. I am lucky to have chance for working with him.

I present my thanks to my colleagues. Special thanks to Güven Yenihayat and Onur Dizdar for their support. I also want to thank my other colleagues Defne Aktaş, Tolga Numanoğlu, Mustafa Kesal, Soner Yeşil, Füruzan Atay Onat, Barış Karadeniz and Halime Koca. Your friendships are irreplaceable. I also want to thank my friends Yadigar Çakmak and Murat Arslan and many others that I forgot to mention their names. They have always tried to help me and shared their experience. It has been a privilege to know such a great group of people.

I appreciate my company ASELSAN for supporting me during my master education.

Last but not least, my deepest gratitude and love to my family. I would love to thank my parents Mustafa and Kıymet, and my brother Kağan. I am very grateful to them. They have been always there whenever I need them to support me during all my education life. I could not have accomplished any of this without them.

TABLE OF CONTENTS

LIST OF TABLES

TABLES

LIST OF FIGURES

FIGURES

LIST OF ABBREVIATIONS

BER	Bit error rate
D-BLAST	Diagonal - Bell Laboratories Layered Space-Time
DVB-T	Digital Video Broadcasting - Terrestrial
FEC	Forward error-correction
FER	Frame error rate
HQAM	Hierarchical quadrature amplitude modulation
LDPC	Low-density parity-check
LLR	Log-likelihood ratio
MAP	Maximum a posteriori
MIMO	Multiple-input multiple-output
ML	Maximum-likelihood
MMSE	Minimum mean square error
MSE	Mean square error
OFDM	Orthogonal frequency division multiplexing
QoS	Quality of service
SIC	Successive interference cancellation
SINR	Signal-to-interference-plus-noise ratio
SISO	Single-input single-output
SNR	Signal-to-noise ratio
STC	Space-time coding
UEP	Unequal error protection
V-BLAST	Vertical - Bell Laboratories Layered Space-Time
WiMAX	Worldwide Interoperability for Microwave Access
ZF	Zero forcing

CHAPTER 1

INTRODUCTION

In wireless communication systems, multiple antennas can be used to increase data rates through spatial multiplexing or to improve transmission reliability through space-time coding (STC). There is a diversity-multiplexing trade-off in multiple input multiple output (MIMO) systems, focusing on obtaining either diversity or multiplexing gain traditionally. STC schemes operate on the diversity end of this trade-off since they attain the maximum avaliable diversity for a single stream. Although STC can provide very reliable transmission, the data rates are limited due to single stream transmission. The focus is on high rate communication in this work so that multiple stream transmission will be studied.

The advantages of using multiple antennas are analyzed by Telatar [1] and it is shown that channel capacity can be increased significantly. MIMO systems can provide high data rates through spatial multiplexing in which independent data streams are sent from different antennas. The first spatial multiplexing techniques were introduced by researchers at Bell Laboratories. The early introduced structure was Diagonal - Bell Laboratories Layered Space-Time (D-BLAST) [2], in which complexity is too high to be practical. It has also an overhead due to the non-transmission in some space-time slots. Vertical-BLAST (V-BLAST) [3] is a simplified version of D-BLAST, but it has lower capacity. The optimal detection method for V-BLAST systems is maximum-likelihood (ML), which has high computational complexity. The complexity increases exponentially with the number of transmit antennas. Complexity can be reduced by linear receivers such as zero forcing (ZF) and linear minimum mean square error (MMSE) receivers. ZF receiver generally has significant performance

degradation due to noise enhancement. MMSE receiver has better performance compared to ZF but the improvement is limited. Decision feedback can be used to improve performance, where detected symbols are canceled and undetected symbols are filtered (either ZF or MMSE filtering). In this work, MMSE is used for filtering the inter-stream interference similar to the V-BLAST receiver. We will call it the successive interference cancellation (SIC) method. Linear receivers with SIC provide a good trade-off between complexity and performance. The error performance with the SIC method is worse than ML but better than linear receivers. The sphere decoding algorithm [4] is another commonly used method to decrease complexity, although it is not discussed in this work due to its worst case complexity of exponential order [5].

Hierarchical modulation consists of two or more standard modulations, which are called layers. The origins of hierarchical modulation can be traced back to Cover's study of broadcast channels [6]. Hierarchical modulation is included in many digital broadcasting standards such as Digital Video Broadcasting - Terrestrial (DVB-T) [7] especially since unequal error protection (UEP) can be provided to different layers. The layer with the highest protection capability is called the base layer and the other layers are called enhancement layers. Therefore the highest priority data is sent over the base layer. The base layer can be decoded even under bad channel conditions, so system robustness is enhanced. Under good channel conditions, both layers can be decoded. Decoding of enhancement layers can be used to increase data rate and provides a good quality of service (QoS) [8].

The main aim of this work is to develop high data rate MIMO systems with low receiver computational complexity. Considering ML and MMSE receivers, a two-stage receiver structure is utilized. Layers with different protection levels are transmitted using hierarchical modulation. Protection levels are designed considering ML and MMSE receivers' error rate performance capabilities. A similar idea is mentioned in [9], where ML is used at both stages of receiver and bit error rate (BER) performance exhibits an error floor. In this work, a new receiver structure is proposed which has a better error rate performance. In the proposed receiver, the base layer is detected first with the MMSE filter which is followed by ML detection of the enhancement layer.

The remainder of this thesis is organized as follows. Chapter 2 introduces the related background that includes MIMO system model and receiver structures, hierarchical 16-ary quadrature amplitude modulation (16-HQAM), block fading channel model and low-density parity-check (LDPC) codes. The proposed receiver structure is described and the computational complexity of the proposed receiver is analyzed in Chapter 3. Results are presented in Chapter 4. Finally, conclusions are drawn in Chapter 5.

Notation: Bold small and capital letters denote vector and matrices, respectively. The superscripts $(\cdot)^{\mathbf{H}}$, $(\cdot)^T$ and $(\cdot)^{-1}$ represent the Hermitian transpose, the transpose and the matrix inverse, respectively. The identity matrix is represented by $\mathbf{I}$. The expectation is denoted by $\mathrm{E}[\cdot]$ and $\|\cdot\|$ denotes Euclidean vector norm. Big-O Notation is denoted by $\mathcal{O}(\cdot)$.

CHAPTER 2

BACKGROUND

2.1 MIMO Systems

This section describes the MIMO system model and explains the transmitter and receiver structures of MIMO systems that will be used in the proposed receiver.

2.1.1 MIMO System Model

A single point-to-point MIMO channel system with N_t transmit and N_r receive antennas can be represented as

$$\mathbf{y} = \frac{1}{\sqrt{N_t}}\mathbf{H}\mathbf{x} + \mathbf{n}, \tag{2.1}$$

where $\mathbf{y}$ is the received complex signal vector, $\mathbf{x}$ is the transmitted complex signal vector with $\mathrm{E}[\mathbf{x}\mathbf{x}^H] = \mathbf{I}$, $\mathbf{n}$ is the vector of independently and identically distributed zero-mean circularly symmetric additive white Gaussian complex noise variables with variance N_0 and $\mathbf{H}$ is the complex channel matrix whose elements have unit variances. Noise variance changes with the relation $N_0 = 1/\mathrm{SNR}$, where SNR is the signal-to-noise ratio. Each column vector of $\mathbf{H}$ is represented by $\mathbf{h_i}$. In this work, the channel $\mathbf{H}$ is perfectly known to the receiver and undergoes flat Rayleigh fading. The total transmitted energy is set to unity and equally shared by transmit antennas. The vectors and the channel matrix $\mathbf{H}$ can be written as follows

$$\mathbf{y} = \begin{bmatrix} y_1 \\ y_2 \\ \vdots \\ y_{N_r} \end{bmatrix}, \quad \mathbf{x} = \begin{bmatrix} x_1 \\ x_2 \\ \vdots \\ x_{N_t} \end{bmatrix}, \quad \mathbf{n} = \begin{bmatrix} n_1 \\ n_2 \\ \vdots \\ n_{N_r} \end{bmatrix},$$

$$\mathbf{H} = \begin{bmatrix} h_{1,1} & h_{1,2} & \dots & h_{1,N_t} \\ h_{2,1} & h_{2,2} & \dots & h_{2,N_t} \\ \vdots & \vdots & \vdots & \vdots \\ h_{N_r,1} & h_{N_r,2} & \dots & h_{N_r,N_t} \end{bmatrix} = \begin{bmatrix} | & | & & | \\ \mathbf{h_1} & \mathbf{h_2} & \dots & \mathbf{h_{N_t}} \\ | & | & & | \end{bmatrix}.$$

Figure 2.1 shows a basic system model of MIMO.

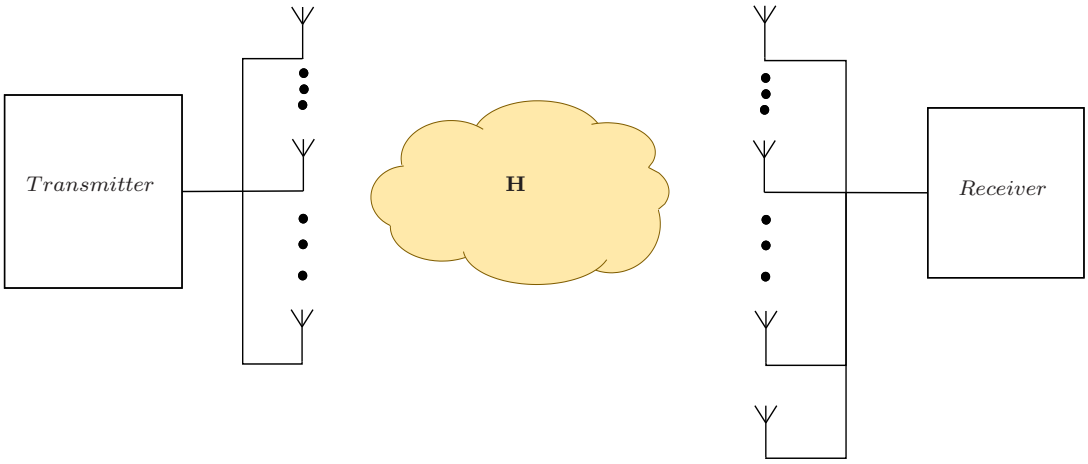

Figure 2.1: MIMO system model

2.1.2 MIMO Transmitter and Receiver Structures

BLAST transmitter structures achieve high data rates since they are spatial multiplexing schemes. Data stream is demultiplexed into substreams and transmitted from different antennas. BLAST structures are named according to how substreams are mapped to antennas. Figure 2.2 shows the mapping how symbols are transmitted from antennas in the V-BLAST scheme. The numbers in the figure show the order of transmitted symbols in the data stream. As observed in figure, independent

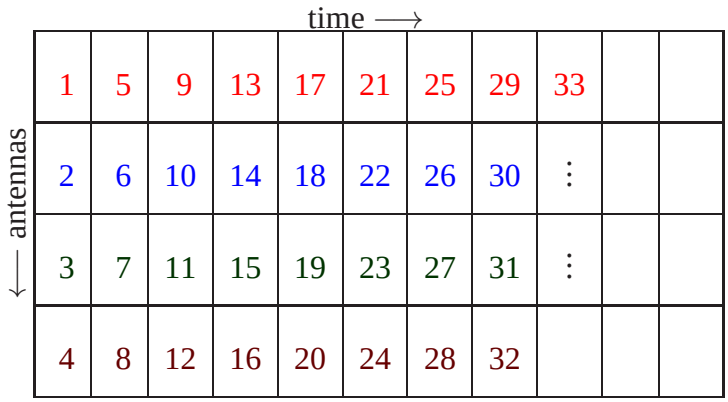

Figure 2.2: Layer mapping in a V-BLAST transmitter

symbols are sent from each antenna in each time slot. V-BLAST is preferred for a simpler transmitter structure in this work at the price of lower capacity compared to D-BLAST. Some of the possible receiver structures of V-BLAST are explained below.

2.1.2.1 ML Receiver

The most generic class of detectors that are designed to minimize the average probability of detection error are called maximum a posteriori (MAP) detectors. The design rule for members of the MAP class is to declare the input vector that has the maximum conditional probability given the observation vector as the estimate. Mathematically speaking, the MAP rule is

$$\begin{aligned}\widehat{\mathbf{x}} &= \arg\max_{\bar{\mathbf{x}}\in\mathbb{A}_{\mathfrak{x}}} \Pr(\bar{\mathbf{x}} \text{ was sent}|\mathbf{y} \text{ is observed}) \\ &= \arg\max_{\bar{\mathbf{x}}\in\mathbb{A}_{\mathfrak{x}}} \frac{\Pr(\mathbf{y} \text{ is observed})|\bar{\mathbf{x}} \text{ was sent}) \Pr(\bar{\mathbf{x}} \text{ was sent})}{\Pr(\mathbf{y} \text{ is observed})} \\ &= \arg\max_{\bar{\mathbf{x}}\in\mathbb{A}_{\mathfrak{x}}} \Pr(\mathbf{y} \text{ is observed})|\bar{\mathbf{x}} \text{ was sent}) \Pr(\bar{\mathbf{x}} \text{ was sent}), \end{aligned} \tag{2.2}$$

where $\mathbb{A}_{\mathfrak{x}}$ is the set of all possible transmitted signal vectors. In the last step of (2.2), we discarded the probability of the observed vector since it does not depend on $\bar{\mathbf{x}}$. It turns out that in most of the practical systems data vectors are equally likely to be transmitted, the optimal decision rule simplifies further to the following form

$$\widehat{\mathbf{x}} = \arg\max_{\bar{\mathbf{x}}\in\mathbb{A}_{\mathfrak{x}}} \Pr(\mathbf{y} \text{ is observed})|\bar{\mathbf{x}} \text{ was sent}), \tag{2.3}$$

which can be defined as the likelihood function. Furthermore, the logarithm function is monotonically increasing, therefore maximizing the likelihood function is equivalent to maximizing the log likelihood function. Hence, an equivalent form of (2.4) can be written as follows

$$\widehat{\mathbf{x}} = \underset{\bar{\mathbf{x}} \in \mathbb{A}_{\mathfrak{x}}}{\arg\max} \ \log \Pr(\mathbf{y} \text{ is observed}) | \bar{\mathbf{x}} \text{ was sent}). \tag{2.4}$$

Specifically for our system formulated in (2.1), the ML decision rule takes the folowing form

$$\begin{aligned} \widehat{\mathbf{x}} &= \underset{\bar{\mathbf{x}} \in \mathbb{A}_{\mathfrak{x}}}{\arg\max} -\frac{1}{N_0} \left\| \mathbf{y} - \frac{1}{\sqrt{N_t}} \mathbf{H} \bar{\mathbf{x}} \right\| \\ &= \underset{\bar{\mathbf{x}} \in \mathbb{A}_{\mathfrak{x}}}{\arg\min} \left\| \mathbf{y} - \frac{1}{\sqrt{N_t}} \mathbf{H} \bar{\mathbf{x}} \right\|. \end{aligned} \tag{2.5}$$

ML detection is a brute-force search over the set $\mathbb{A}_{\mathfrak{x}}$ with a size of M^{N_t} in this setting.

2.1.2.2 ZF Receiver

The ZF receiver class enables another detection mechanism which aims to remove the contribution of the channel matrix $\mathbf{H}$ on the transmitted vector [10]. In other words, the channel output vector is multiplied by the pseudo-inverse of the channel matrix scaled by $\sqrt{N_t}$. The ZF filter is given by

$$\mathbf{W}^{\mathbf{H}} = \sqrt{N_t} (\mathbf{H}^{\mathbf{H}} \mathbf{H})^{-1} \mathbf{H}^{\mathbf{H}}. \tag{2.6}$$

Using the received vector expression given by (2.1), the ZF filtered channel output is in the following form

$$\mathbf{z} = \mathbf{W}^{\mathbf{H}} \mathbf{y} = \mathbf{x} + \sqrt{N_t} (\mathbf{H}^{\mathbf{H}} \mathbf{H})^{-1} \mathbf{H}^{\mathbf{H}} \mathbf{n}. \tag{2.7}$$

As observed in (2.7), the noise may be amplified for some random channels which may result in a poor ZF detector performance. In order to alleviate this drawback, an MMSE equalizer is proposed to improve the performance of the receiver. In this design, both the ISI mitigation and the channel noise impairments are targetted simultaneously so as to get a better receiver performance as described in the next section.

2.1.2.3 MMSE Receiver

MMSE filter is designed to minimize mean square error (MSE). In other words, it minimizes the total error due to the combination of noise and distortion. The received signal is passed through the MMSE receiver. The filter output is given by

$$\mathbf{z} = \mathbf{W^H y}, \tag{2.8}$$

where $\mathbf{W^H}$ represents MMSE equalization filter. The mean square error in the filter output is computed for the transmitted signal vector as

$$\begin{aligned} J &= \mathrm{E}[\|\mathbf{z} - \mathbf{x}\|^2] \\ &= \mathrm{E}[\|\mathbf{W^H y} - \mathbf{x}\|^2] \\ &= \mathrm{E}\left[(\mathbf{W^H y} - \mathbf{x})^{\mathbf{H}}(\mathbf{W^H y} - \mathbf{x})\right] \\ &= \mathrm{E}\left[(\mathbf{y^H W} - \mathbf{x^H})(\mathbf{W^H y} - \mathbf{x})\right] \\ &= \mathrm{E}\left[\mathbf{y^H W W^H y} - \mathbf{y^H W x} - \mathbf{x^H W^H y} + \mathbf{x^H x}\right]. \end{aligned} \tag{2.9}$$

The MMSE equalization filter is found by minimizing J in (2.9), where $\mathbf{W}$ is chosen such that it makes the first derivative of J equals 0.

$$\begin{aligned} 0 &= \frac{\partial J}{\partial \mathbf{W}} \\ &= \mathrm{E}\left[\frac{\partial}{\partial \mathbf{W}}\left(\mathbf{y^H W W^H y} - \mathbf{y^H W x} - \mathbf{x^H W^H y} + \mathbf{x^H x}\right)\right] \\ &= \mathrm{E}\left[(\mathbf{y^H y} + \mathbf{y^H y})\mathbf{W} - \mathbf{y x^H} - \mathbf{y x^H}\right]. \end{aligned} \tag{2.10}$$

Before we proceed, we provide certain matrix derivative properties that are essential for our derivations. Given the column vectors $\mathbf{a}$ and $\mathbf{b}$ with respective lengths M and N, let $\mathbf{X}$ be a matrix of dimensions $M \times N$. Then

$$\begin{aligned} \frac{\partial \mathbf{a^H X b}}{\partial \mathbf{X}} &= \mathbf{a b^H} \\ \frac{\partial \mathbf{a^H X^H b}}{\partial \mathbf{X}} &= \mathbf{b a^H} \\ \frac{\partial \mathbf{a^H X X^H b}}{\partial \mathbf{X}} &= \mathbf{a}(\mathbf{X^H b})^{\mathbf{H}} + \mathbf{b a^H X} = (\mathbf{a b^H} + \mathbf{b a^H})\mathbf{X}. \end{aligned}$$

For a detaied treatment, see [11].

By continuing (2.10), minimisation of J leads to the Wiener-Hopf equation as

$$\begin{aligned} 2\mathrm{E}\left[\mathbf{y}\mathbf{y}^{\mathbf{H}}\right]\mathbf{W} - 2\mathrm{E}\left[\mathbf{y}\mathbf{x}^{\mathbf{H}}\right] &= 0 \\ \mathrm{E}\left[\mathbf{y}\mathbf{y}^{\mathbf{H}}\right]\mathbf{W} &= \mathrm{E}\left[\mathbf{y}\mathbf{x}^{\mathbf{H}}\right] \\ \mathbf{W}^{\mathbf{H}}\mathrm{E}\left[\mathbf{y}\mathbf{y}^{\mathbf{H}}\right] &= \mathrm{E}\left[\mathbf{x}\mathbf{y}^{\mathbf{H}}\right] \\ \mathbf{W}^{\mathbf{H}} &= \mathrm{E}\left[\mathbf{x}\mathbf{y}^{\mathbf{H}}\right]\left(\mathrm{E}\left[\mathbf{y}\mathbf{y}^{\mathbf{H}}\right]\right)^{-1}. \end{aligned} \tag{2.11}$$

MMSE equalization filter can be found by solving (2.11). We refer (2.11) as MMSE filter equation in this work and it will be used in the next chapter to find MMSE filters for the proposed structure. Finally $\mathbf{W}^{\mathbf{H}}$ is found as

$$\begin{aligned} \mathbf{W}^{\mathbf{H}} &= \mathrm{E}\left[\mathbf{x}\left(\frac{1}{\sqrt{N_t}}\mathbf{x}^{\mathbf{H}}\mathbf{H}^{\mathbf{H}} + \mathbf{n}^{\mathbf{H}}\right)\right]\left\{\mathrm{E}\left[\left(\frac{1}{\sqrt{N_t}}\mathbf{H}\mathbf{x} + \mathbf{n}\right)\left(\frac{1}{\sqrt{N_t}}\mathbf{x}^{\mathbf{H}}\mathbf{H}^{\mathbf{H}} + \mathbf{n}^{\mathbf{H}}\right)\right]\right\}^{-1} \\ &= \frac{1}{\sqrt{N_t}}\mathbf{H}^{\mathbf{H}}\left(\frac{1}{N_t}\mathbf{H}\mathbf{H}^{\mathbf{H}} + N_0\mathbf{I}\right)^{-1}. \end{aligned} \tag{2.12}$$

The MMSE receiver decouples a MIMO system into SISO systems and decisions are made on each filter output $\mathbf{z} = [z_1, ..., z_{N_t}]^T$ as

$$\widehat{x}_i = \underset{\bar{x}\in\mathbb{A}_{\mathfrak{X}}}{\arg\min} \|z_i - \bar{x}\|, \tag{2.13}$$

where $\mathbb{A}_{\mathfrak{X}}$ is the set of constellation points.

2.1.2.4 MMSE-SIC Receiver

MMSE receiver can be used with the SIC method to enhance performance. MMSE-SIC receiver can be considered as an MMSE receiver with a decision feedback mechanism. Its operation is recursive in nature, each step is based on the following three steps:

1. Filtering to minimize interference-plus-noise term,
2. Ordering to select the symbol with the highest signal-to-interference-plus-noise ratio (SINR),
3. Canceling the symbol which has the highest SINR.

A new filter is designed for the remaining signals and these steps are repeated until all symbols are detected. It is referred as ordered successive interference cancellation

(OSIC) or V-BLAST receiver structure in the literature [3]. It will be called MMSE-SIC receiver in this work. The architecture is illustrated in Figure 2.3.

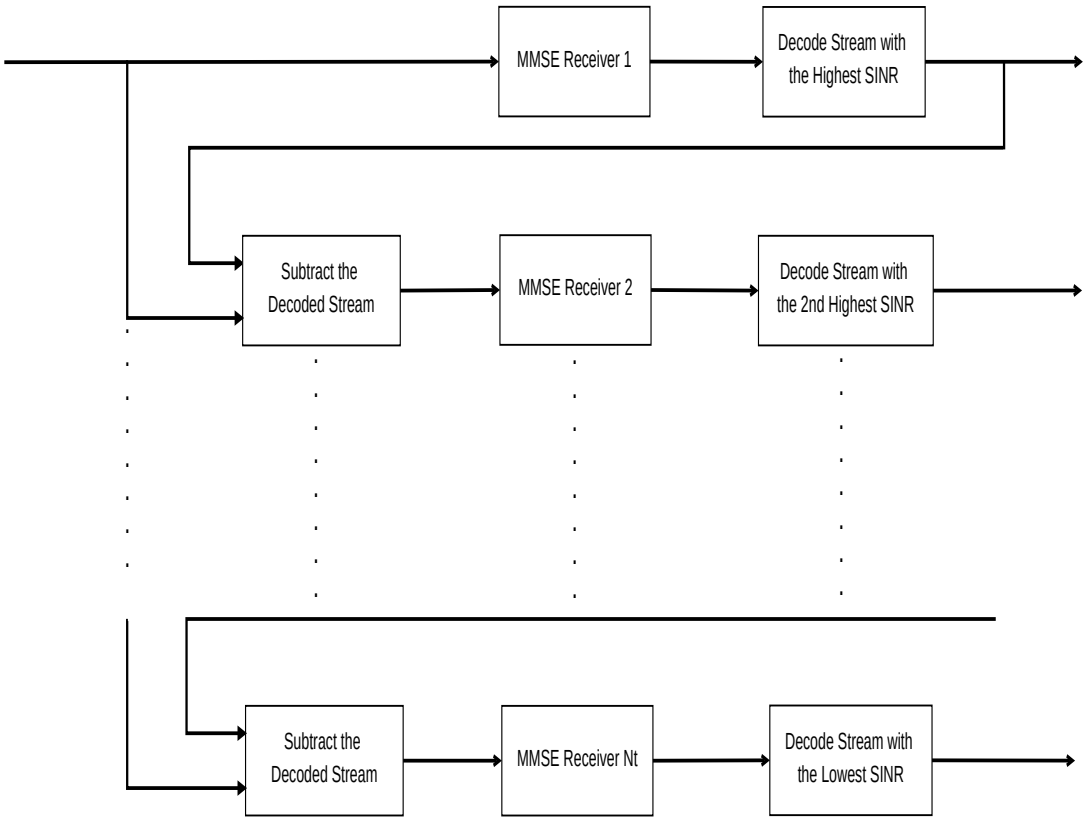

Figure 2.3: The architecture of MMSE-SIC receiver

Figure 2.4 underlies the importance of canceling the symbol with the highest SINR. In the figure, 4×4 MIMO BER performances of MMSE, MMSE with OSIC and MMSE with fixed order SIC (i.e. cancellation order: 1st, 2nd, 3rd, 4th antenna) are shown for 16-QAM modulated signals. As observed, order of cancellation is critically important for achieving significant performance enhancement. Fixed order cancellation has a limited performance improvement compared to the MMSE receiver.

The Hermitian transpose of MMSE filter in (2.12) is written as

$$\mathbf{W} = \begin{bmatrix} | & | & & | \\ \mathbf{g_1} & \mathbf{g_2} & \cdots & \mathbf{g_{N_t}} \\ | & | & & | \end{bmatrix}, \tag{2.14}$$

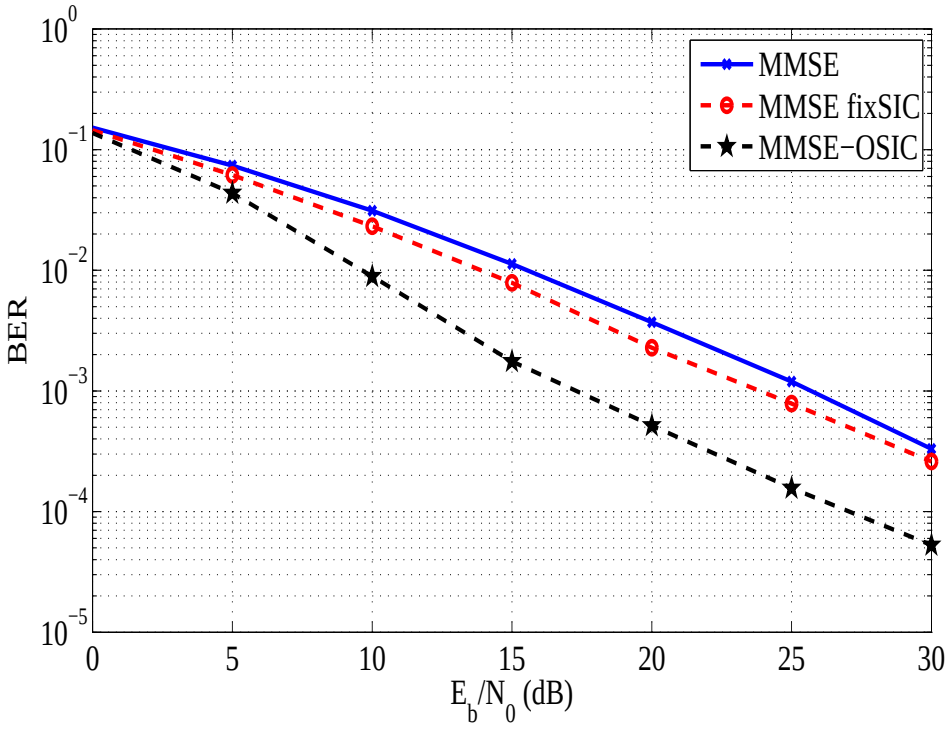

Figure 2.4: Effect of the order of cancellation

where $\mathbf{g_i}$ is the filter vector which produces the i-th output of MMSE filter. The filter vector is represented as

$$\mathbf{g_i} = \frac{1}{\sqrt{N_t}} \left(\frac{1}{N_t} \mathbf{H}\mathbf{H}^{\mathbf{H}} + N_0 \mathbf{I} \right)^{-1} \mathbf{h_i}. \tag{2.15}$$

Passing received vector through the filter vectors yields

$$z_i = \mathbf{g_i^H} \mathbf{y} = \beta_i x_i + \eta_i, \tag{2.16}$$

where β_i is the desired signal term represented as

$$\beta_i = \frac{1}{\sqrt{N_t}} \mathbf{g_i^H} \mathbf{h_i} \tag{2.17}$$

and the interference-plus-noise term is represented as

$$\eta_i = \sum_{k \neq i} \frac{1}{\sqrt{N_t}} \mathbf{g_i^H} \mathbf{h_k} x_k + \mathbf{g_i^H} \mathbf{n}. \tag{2.18}$$

As seen in (2.18), the signals from other antennas are considered as interference. The interference-plus-noise term is modeled as a complex Gaussian random variable. SINR of the i-th signal is written as

$$\mathrm{SINR}_i = \frac{\mathrm{E}[|\beta_i x_i|^2]}{\mathrm{E}[|\eta_i|^2]}. \tag{2.19}$$

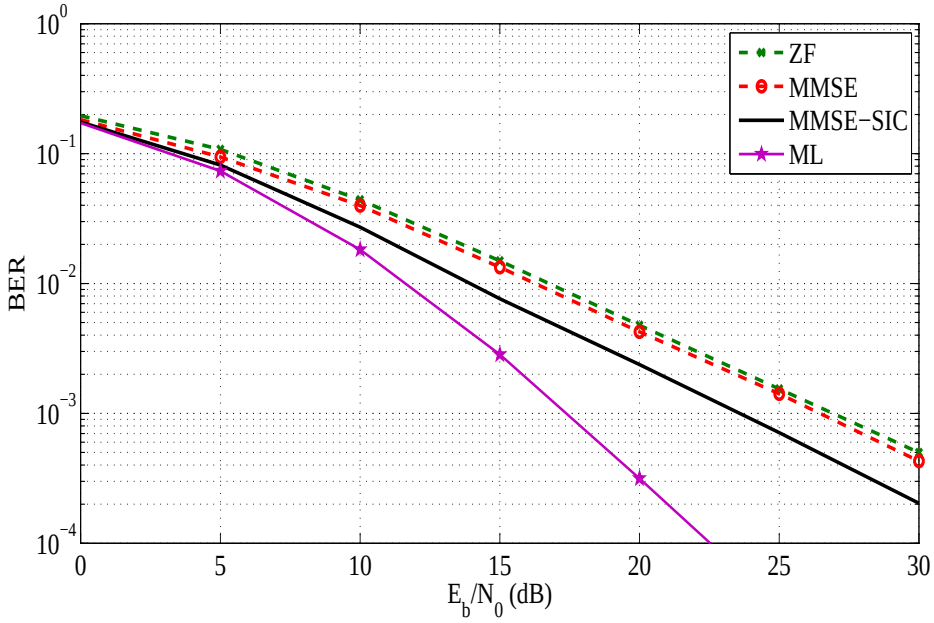

Figure 2.5: Uncoded 2×2 system performance comparison of receivers

Let us consider that the k-th signal has the highest SINR at the MMSE filter output. After detection and assuming perfect cancellation, the rest of the signal vector is written as

$$\tilde{\mathbf{y}} = \frac{1}{\sqrt{N_t}}\tilde{\mathbf{H}}\tilde{\mathbf{x}} + \mathbf{n}, \tag{2.20}$$

where

$$\tilde{\mathbf{H}} = \begin{bmatrix} | & & | & | & & | \\ \mathbf{h_1} & \dots & \mathbf{h_{k-1}} & \mathbf{h_{k+1}} & \dots & \mathbf{h_{N_t}} \\ | & & | & | & & | \end{bmatrix} \quad \text{and} \quad \tilde{\mathbf{x}} = \begin{bmatrix} x_1 \\ \vdots \\ x_{k-1} \\ x_{k+1} \\ \vdots \\ x_{N_t} \end{bmatrix}$$

represent the new channel matrix and the remaining base layer vector that is formed by removing the k-th column of $\mathbf{H}$ and the k-th row of $\mathbf{x}$, respectively. The new MMSE filter designed for vector $\tilde{\mathbf{x}}$ is

$$\tilde{\mathbf{W}}^{\mathbf{H}} = \frac{1}{\sqrt{N_t}}\tilde{\mathbf{H}}^{\mathbf{H}}\left(\frac{1}{N_t}\tilde{\mathbf{H}}\tilde{\mathbf{H}}^{\mathbf{H}} + N_0\mathbf{I}\right)^{-1}. \tag{2.21}$$

Figure 2.5 shows a 2×2 uncoded BER performance comparison of ML, ZF, MMSE and MMSE-SIC receivers for 16-QAM modulation. As it is observed in the figure, error performance of the MMSE-SIC is worse than ML but better than linear receivers (MMSE, ZF).

2.2 Hierarchical 16 QAM

Hierarchical 16-ary quadrature amplitude modulation (16-HQAM) [12] is used in this work. Gray-mapped constellation diagram of 16-HQAM is shown in Figure 2.6. The first two bits indicate the base layer and the last two indicate the enhancement layer. The average power of constellation points is set to unity. The minimum distance of base layer constellation points is represented by d_1 and the minimum distance of enhancement layer constellation points is represented by d_2. The ratio $d = d_1/d_2$ is called the constellation ratio. For the case $d = 2$, the constellation corresponds to

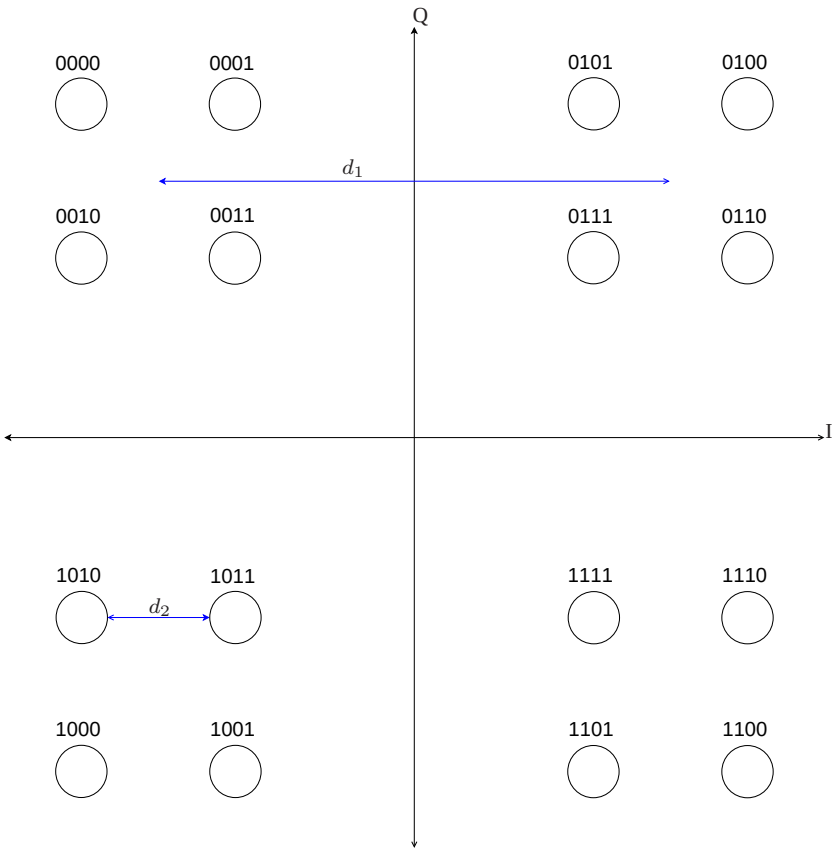

Figure 2.6: Hierarchical 16-QAM Constellation Diagram

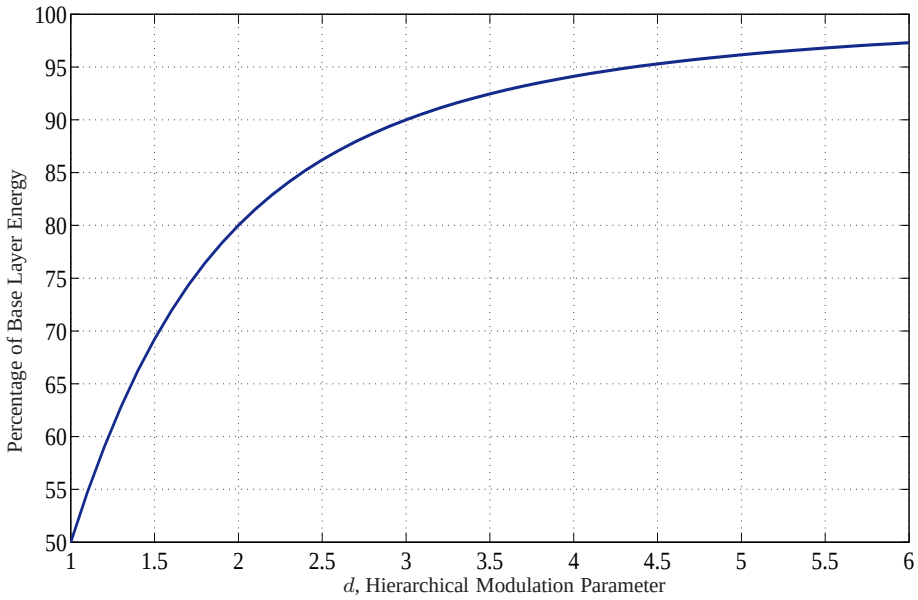

Figure 2.7: Percentage of Transmitted Base Layer Energy

that of standard 16-QAM. The ratio d has to be greater than 1 ($d > 1$), otherwise the constellation points would intersect.

Protection levels of layers can be arranged by changing d. When d is increased:

- Base layer points become more separated and enhancement layer points get closer.
- More energy is transmitted with the base layer, meanwhile, the enhancement layer is sent with less energy. How the percentage of transmitted energy of the base layer changes with the constellation ratio d is illustrated in Figure 2.7.
- The base layer has higher protection and enhancement layer's protection is decreased.

For the single-input and single-output (SISO) case, the BER performance of 16-HQAM is shown in Fig. 2.8. As observed in the figure, there is a trade-off between the performances of base and enhancement layers.

Let us consider detection of hierarchical modulation in a SISO system. The base layer is detected first. Performance is determined by signal-to-interference-plus-noise ratio

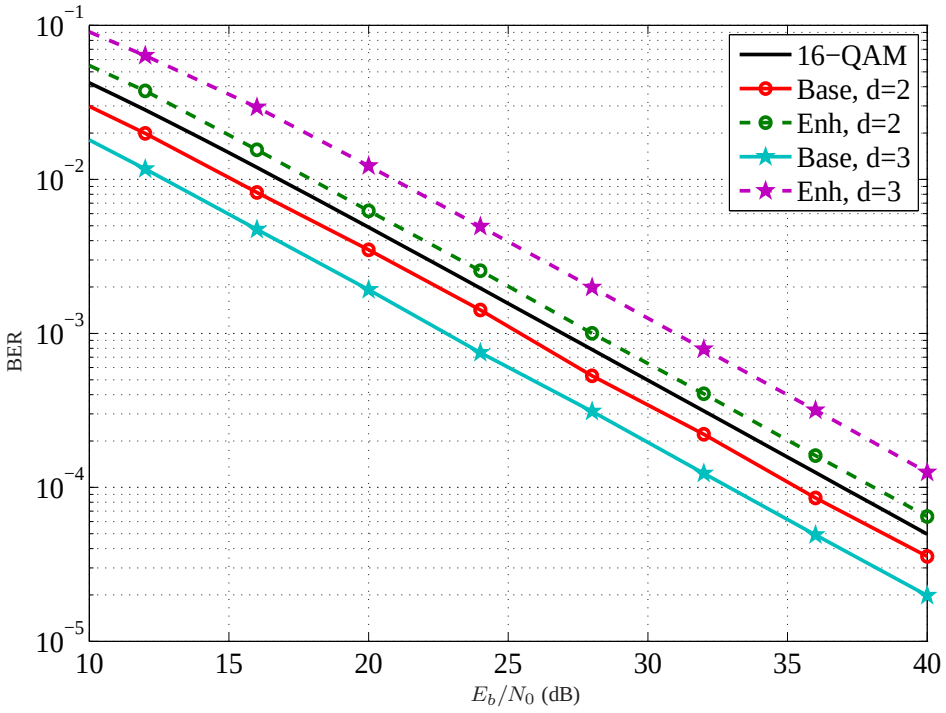

Figure 2.8: BER for uncoded SISO, 16-QAM and 16-HQAM

(SINR) at the base layer due to fact that enhancement layer acts as interference since the first stage detector does not mitigate the effect of enhancement layer. We may regard this SINR as the effective SNR of the base layer. SINR of the base layer can be found as

$$\mathrm{SINR}_{base} = E_{x_b}/(E_{x_e} + N_0), \tag{2.22}$$

where E_{x_b} and E_{x_e} are the energies of the base and enhancement layers, respectively. After detecting the base layer, its effect is canceled in the received signal assuming perfect cancellation, the enhancement layer is only affected by a noise term where SNR becomes the parameter affecting the performance and written as

$$\mathrm{SNR}_{enh} = E_{x_e}/N_0. \tag{2.23}$$

Figure 2.9 gives an idea for the effective SNR on both layers as symbol SNR of 16-HQAM symbols vary. Qualitatively deduce from this figure that when d increases, the base layer will have a better performance whereas the enhancement layer will have worse. One may note based on (2.22) that effective SNR of the base layer does not linearly increase as symbol SNR increases since the energy of enhancement layer

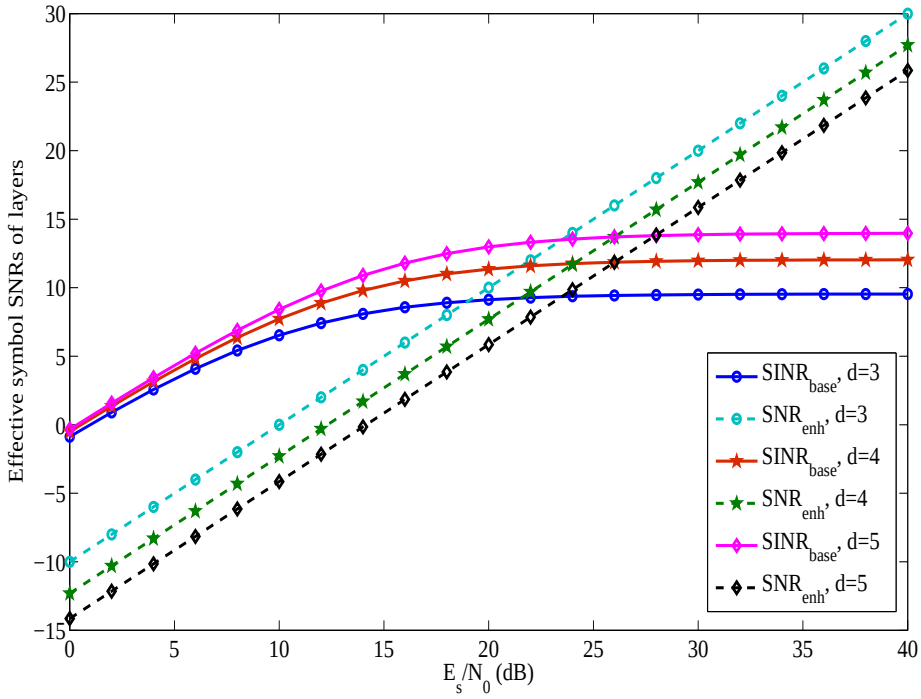

Figure 2.9: Effective SNRs

acting as interference also increases. Given a particular of d, the effective SNR of the base layer has an asymptote that can be calculated based on the constellation diagram as depicted in Figure 2.6.

2.3 Channel Model

The starting point of channel characterization is the equivalent low pass time-varying channel impulse response $c(\tau, t)$, where t is the time variation parameter and τ is the path delay parameter [13]. The Fourier transform of $c(\tau, t)$ with respect to t

$$S_c(\tau, \lambda) = \int_{-\infty}^{\infty} c(\tau, t) e^{-j2\pi\lambda t} dt, \tag{2.24}$$

where $S_c(\tau, \lambda)$ is called scattering function and λ is the frequency parameter. From scattering function, the delay power spectrum of channel can be obtained by averag-

ing $S_c(\tau, \lambda)$ over λ

$$S_c(\tau) = \int_{-\infty}^{\infty} S_c(\tau, \lambda) d\lambda. \tag{2.25}$$

Similarly, the Doppler power spectrum of channel is obtained by averaging $S_c(\tau, \lambda)$ over τ

$$S_c(\lambda) = \int_{-\infty}^{\infty} S_c(\tau, \lambda) d\tau. \tag{2.26}$$

The range of values over which the delay power spectrum $S_c(\tau)$ is nonzero is defined as the multipath delay spread T_m. Similarly, the range of values over which the Doppler power spectrum $S_c(\lambda)$ is nonzero is defined as the Doppler spread B_d. Figure 2.10 illustrates the multipath delay spread and the Doppler spread.

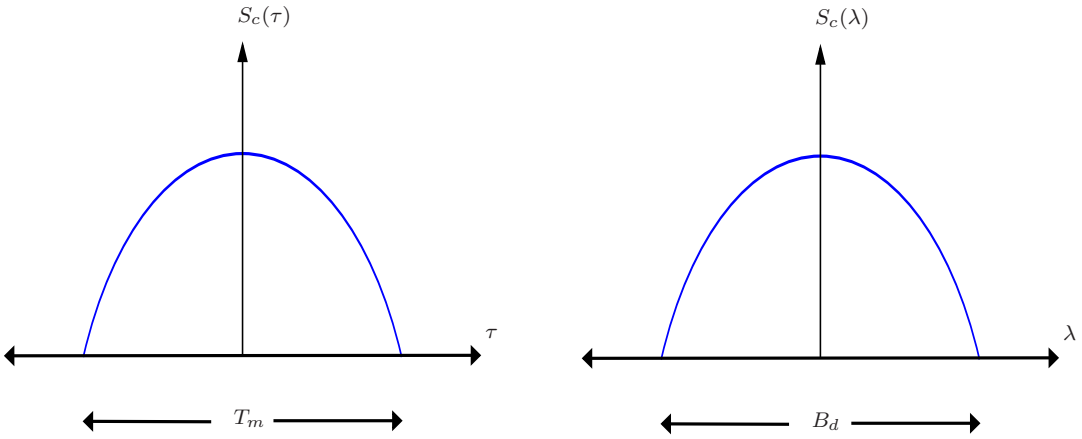

Figure 2.10: The multipath delay spread and the Doppler spread

The Doppler spread B_d is a measure of how rapidly the channel changes with time. A larger B_d leads to more rapid change. The channel coherence time T_c is defined as

$$T_c = \frac{1}{B_d}. \tag{2.27}$$

It can be seen from (2.27), a slowly changing channel has large coherence time. The other channel parameter, called the channel coherence bandwidth B_c is defined as

$$B_c = \frac{1}{T_m}. \tag{2.28}$$

The multipath spread B_c gives the information about the range of frequencies over which amplitude correlation remains high.

The bandwidth of transmitted signal is represented by B and the signal duration is represented by T_s. The relation $T_s \approx 1/B$ exists in linear modulations. For the case $B_c >> B$, or equivalently $T_m << T_s$, the signal experience same amplitude and phase through the channel. This is referred as flat-fading or narrow band or frequency-nonselective channel. If the signal bandwidth is much greater than the Doppler spread ($B >> B_d$), the effects of Doppler spread are negligible at the receiver. Equivalently, $T_s << T_c$. This channel is said to be slow fading.

A narrow band, slow fading channel is assumed in the remainder of this thesis.

2.3.1 Diversity Domains

In wireless telecommunication systems, diversity is a critical issue since it may help to provide safe communication and improve the reception of signals. Diversity can be attained with different techniques. Some of the major diversity domains are described below.

- **Time Diversity:** Diversity over time can be obtained via appropriate coding and interleaving. Coded bits are dispersed over time in different coherence periods so that different parts of codewords experience independent fades.

- **Frequency Diversity:** If the channel is frequency-selective, channel influences different parts of the signal diversely. Frequency diversity can be introduced by transmitting signal in several frequency carriers separated by at least the coherence bandwidth of the channel.

- **Space Diversity:** If the diversity is provided by spatially separated antennas, e.g., MIMO systems, this is know as space diversity. For sufficiently large antenna separations, the channels can be assumed to be independent. Different channel realizations are experienced by signals, so that diversity is obtained.

- **Polarization Diversity:** If antennas support different polarizations, this can be used for polarization diversity. However, this type of diversity is out of covarage in this work.

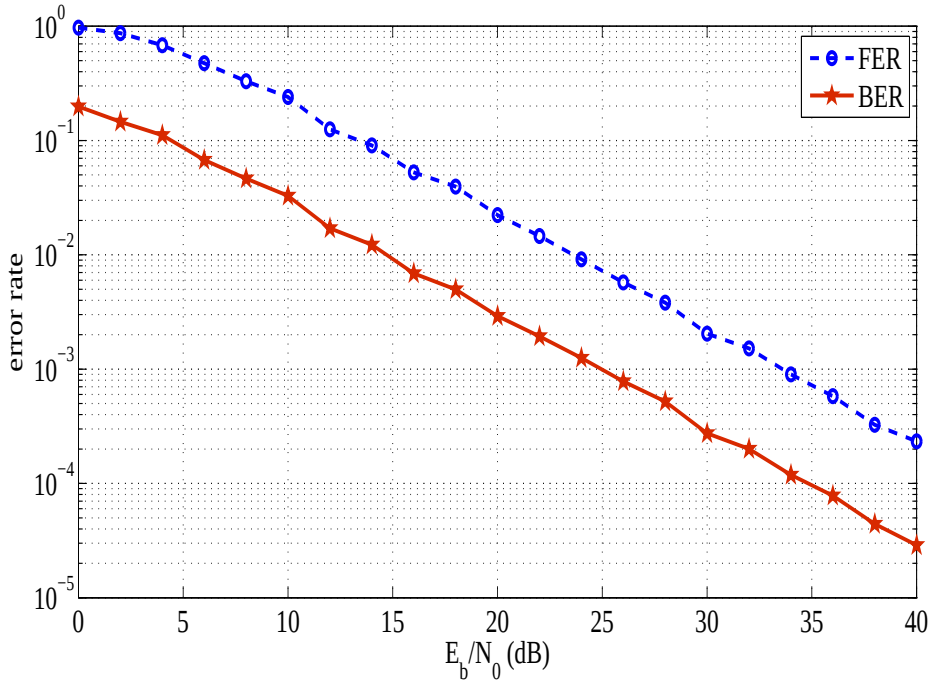

Figure 2.11: One order of diversity, single block transmission over a 2×2 channel, MMSE receiver

2.3.2 Block Fading Channels

Let us explain first the motivation of using the block fading channel model. Under a V-BLAST transmitter structure, MMSE receiver always has diversity $N_r - N_t + 1$, where N_t is the number of transmit antennas and N_r is the number of receiver antennas [14]. This result suggests spatial diversity is not obtained for the case $N_t = N_r$. Without diversity in another domain, diversity with MMSE receiver is then limited to unity. Figure 2.11 illustrates the mentioned diversity order problem. Randomly generated bits are encoded with $R = 3/4$ WiMAX LDPC code with code length 2304 bits and modulated to 16-QAM symbols which are transmitted over a 2×2 MIMO channel that stays constant over entire LDPC block. Finally, bits are detected with MMSE receiver. It is observed from the slopes of error performance curves that diversity order is equal to unity, even with a near Shannon limit code like LDPC. However, when coding over multiple independently fading blocks is present, one can obtain some level of diversity. Hence, a block fading channel model [15] is utilized to achieve diversity with an MMSE receiver in this work.

In the block fading channel model, the encoded bits are combined into a frame. A single frame is separated to F blocks that can be transmitted over different time slots or different frequencies, therefore, time diversity or frequency diversity can be obtained, respectively. Channels are constant within a block and change independently between blocks, which is a valid assumption for various communication systems. In this work, a model considered such that a frame transmitted over different carrier frequencies. The block fading model is relevant for slow frequency hopping systems and multi-carrier modulation systems such as those using orthogonal frequency division multiplexing (OFDM).

2.4 LDPC Codes

LDPC codes are a class of forward error-correction (FEC) linear block codes, first introduced by Robert Gallager in his PhD thesis in 1962 [16]. These codes were ignored many years since they were impractical due to their high computational demands for those years. The FEC codes have been dominated by convolutional codes until the emergence of turbo codes. There was a big gap between the Shannon limit and performance limits of convolutional codes. Turbo codes near Shannon limit were introduced by Berrou, Glavieux and Thitimajshima in 1993. Researchers have been trying to find out why turbo codes worked well and those researches led to rediscovery of LDPC codes [17]. They are practical and very promising with the processing power available today.

LDPC codes are constructed by sparse parity check matrices. The name comes from the characteristic of their parity-check matrix which contains only a few ones in comparison to the amount of zeros. A graphical description of parity check matrix can be expressed with Tanner Graphs. It contains variable and check nodes. Figure 2.12 provides an example of Tanner Graph for the parity check matrix

$$\mathbf{P} = \begin{bmatrix} 1 & 1 & 0 & 1 & 0 & 0 & 1 & 0 \\ 0 & 1 & 1 & 0 & 0 & 1 & 0 & 0 \\ 0 & 0 & 0 & 1 & 0 & 1 & 0 & 1 \\ 1 & 0 & 0 & 0 & 1 & 0 & 1 & 0 \end{bmatrix}.$$

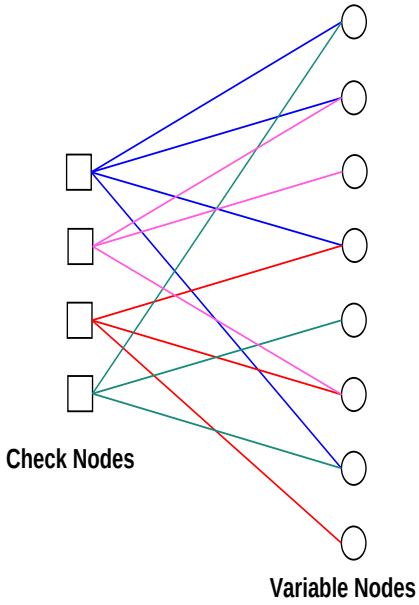

Figure 2.12: Tanner Graph

LDPC codes with very high code lengths are used in many digital TV standards such as Digital Video Broadcasting - Satellite (DVB-S), - Terrestrial (DVB-T) and - Cable (DVB-C). For example, DVB-S2 presents codes of length 16200 and 64800 bits with 11 different code rates. LDPC codes are also used in wireless application standards such as 802.16e Worldwide Interoperability for Microwave Access (WiMAX) and 802.11n Wireless Fidelity (WiFi).

Some advantages of LDPC codes compared to turbo codes are given as:

- The decoding complexity of LDPC codes per iteration is much lower.
- LDPC codes have a great implementation advantage since they are parallelizable.
- LDPC codes can be designed for almost any rates and block length, simply changing the size of parity check matrix. On the other hand, different rates of turbo codes can be obtained by puncturing which needs a design effort to find puncturing patterns.
- There is no need for an interleaver block since interleaving is intrinsic in the LDPC. Hence deinterleaver is also not needed in the system.

The main disadvantage is the LDPC encoders are more complex than turbo encoders,

although there are so many studies and progress in lower complexity LDPC encoders.

2.4.1 LDPC Encoder

The parity-check matrices $\mathbf{P}$ of WiMAX LDPC codes are in the standard form and they can be written in the form

$$\mathbf{P} = [\mathbf{A}, \mathbf{I_{k-n}}], \tag{2.29}$$

where $\mathbf{A}$ is an $(n-k)\times k$ binary matrix and $\mathbf{I_{k-n}}$ is the $k-n\times k-n$ identity matrix. The generator matrix can be written as

$$\mathbf{G} = [\mathbf{I_k}, \mathbf{A^T}]. \tag{2.30}$$

Note that the parity-check matrix and the generator matrix fit the equation

$$\mathbf{GP^T} = \mathbf{0}. \tag{2.31}$$

The message signal $\mathbf{m}$ is encoded by multiplying with the generator matrix as

$$\mathbf{c} = \mathbf{Gm}. \tag{2.32}$$

2.4.2 LDPC Decoder

Different researchers come up with independently more or less the same iterative decoding algorithm, named the belief propagation algorithm, the message passing algorithm or the sum-product algorithm. The Tanner Graph can be used to explain the decoding algorithm.

The sum-product decoding algorithm steps are explained below.

The i-th check node and the j-th variable node are represented by c_i and v_j, respectively. The message passed from the i-th check node to the j-th variable node is denoted by $\beta_{c_i\to v_j}$ and the message passed from the j-th variable node to the i-th check node is represented by $\mu_{v_j\to c_i}$.

- ***Step 0:*** Variable nodes are initialized with the LLR values given to the LDPC decoder. The channel observation vector $\mathbf{y}$ is used to generate soft information in the form of log-likelihood ratio (LLR) which is defined as

$$LLR_l = \ln \frac{\Pr(b^l = 1|\mathbf{y}, \mathbf{H})}{\Pr(b^l = 0|\mathbf{y}, \mathbf{H})}.$$

The number of iteration donated by N_{itt} is set to 1.

$$\begin{aligned} \mu_{v_l \to c_k} &= LLR_l && \forall l, k \\ \beta_{c_k \to v_l} &= 0 && \forall l, k \\ N_{itt} &= 1 \end{aligned}$$

- ***Step 1:*** Check nodes are updated.

$$\beta_{c_i \to v_j} = 2 \tanh^{-1} \left(\prod_{j' \in L(i) \backslash j} \tanh \left(\frac{1}{2} \mu_{v_{j'} \to c_i} \right) \right)$$

where $L(i)$ is the index of variable nodes that are connected to the i-th check node. ($L(i) = \{l | h_{i,l} = 1\}$)

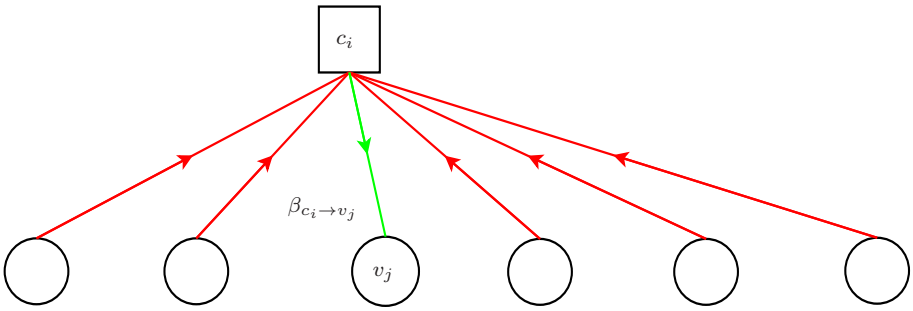

Figure 2.13: Step 1 of Sum-Product Decoding Algorithm

- ***Step 2:*** Variable nodes are updated with this rule

$$\mu_{v_j \to c_i} = \mu_{v_j} + \sum_{i' \in M(j) \backslash i} \beta_{c_{i'} \to v_j}$$

where $M(j)$ is the index of check nodes that are connected to the i-th variable node. ($M(j) = \{k | h_{k,j} = 1\}$)

- ***Step 3:*** Variable nodes are updated.

$$\mu_{v_j} = \mu_{v_j} + \sum_{k' \in M(j)} \mu_{c_{k'} \to v_j}$$

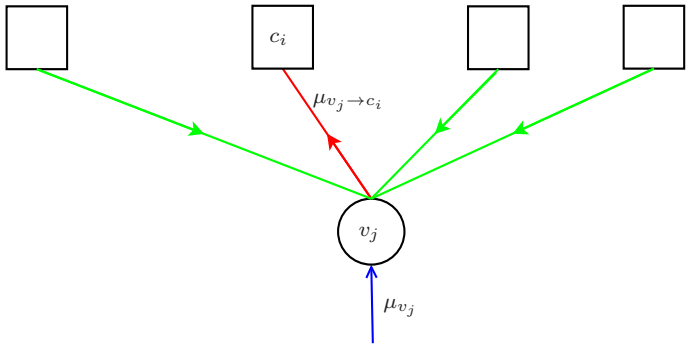

Figure 2.14: Step 2 of Sum-Product Decoding Algorithm

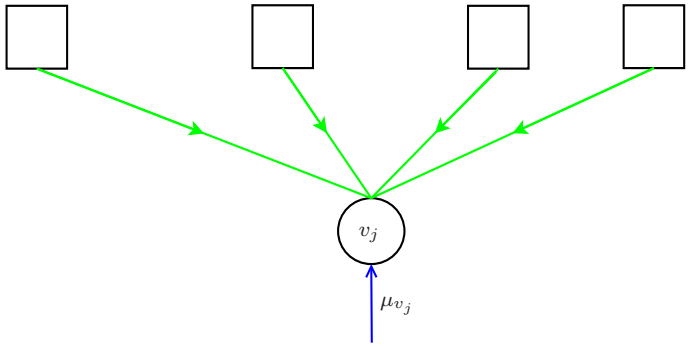

Figure 2.15: Step 3 of Sum-Product Decoding Algorithm

- ***Step 4:*** Hard decisions are given based on the latest soft values at variable nodes.

$$\hat{m}_j = \begin{cases} 0 & \text{if} \quad \mu_{v_j} < 0 \\ 1 & \text{if} \quad \mu_{v_j} \geq 0 \end{cases}$$

- ***Step 5:*** Checking stopping criteria: If parity check equation is satisfied, decoding is terminated. Otherwise, steps are repeated until the termination criteria is obtained or until the maximum number of iterations N_{max} is reached. Unless the parity check equation is satisfied at the maximum number of iterations, decoder can indicate an error. Algorithm can be summarized as

$$\begin{cases} \text{Satisfied stopping criteria} & \text{if} \quad \mathbf{P}\hat{\mathbf{m}} = \mathbf{0} \quad \text{and} \quad N_{itt} \leq N_{max} \\ N_{itt} = N_{itt} + 1 \text{ and go Step 1} & \text{if} \quad \mathbf{P}\hat{\mathbf{m}} \neq \mathbf{0} \quad \text{and} \quad N_{itt} < N_{max} \\ \text{Failure} & \text{if} \quad \mathbf{P}\hat{\mathbf{m}} \neq \mathbf{0} \quad \text{and} \quad N_{itt} = N_{max} \end{cases}$$

In this work, WiMAX LPDC codes are used due to their proper code rates and code lengths. More details of WiMAX LDPC codes are provided in Appendix A where how to create parity check matrix for given rate and code length are explained.

CHAPTER 3

THE PROPOSED RECEIVER STRUCTURE

In this chapter, we will first explain the structure of the proposed receiver for the uncoded and coded cases. Then, computational complexities will be analyzed. The complexity of the proposed strucutre will be compared with the ML and MMSE receivers, which are introduced in Chapter 2.

We are motivated by the fact that the ML receiver has good error rate performance at the price of high computational complexity which increases exponentially with the number of antennas. This is a big problem if high number antennas are necessary in the communication system. One of the common way to decrease the complexity is using MMSE receiver. However, it may cause a poor error rate performance. There is a trade-off between performance and complexity. In this chapter, we propose a receiver which provides favorable gains in both complexity and performance of the system.

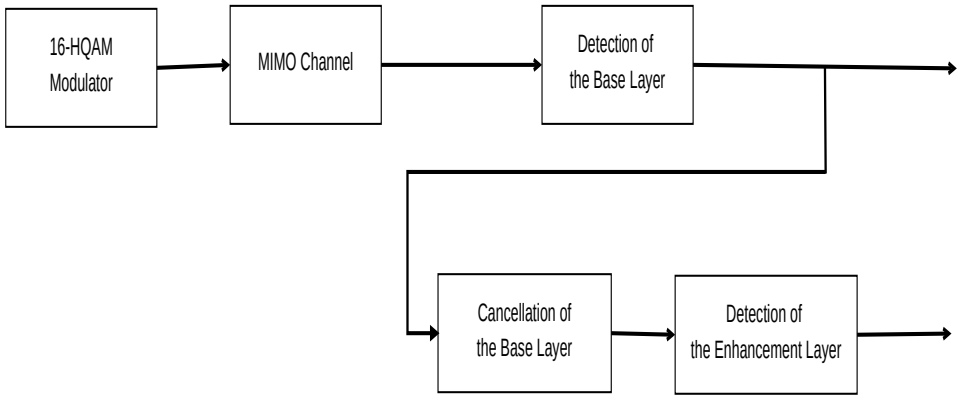

Figure 3.1: System Structure

The proposed receiver structure for the MIMO system using hierarchical modulation works sequentially. First, the base layer is decoded which is followed by detection of the enhancement layer. System structure is shown in Figure 3.1 The case for which MMSE receiver is used for the base layer and ML receiver is used for the enhancement layer performs the best with comparison to the other cases such as ML or MMSE detection at both layers. The reason why it has the best performance will be explained later in Chapter 4.

The transmitted vector $\mathbf{x}$ can be written as the sum of the base layer vector and enhancement layer vector, $\mathbf{x} = \mathbf{x_b} + \mathbf{x_e}$. The system model (2.1) can be rewritten as

$$\mathbf{y} = \frac{1}{\sqrt{N_t}}\mathbf{H}\mathbf{x_b} + \frac{1}{\sqrt{N_t}}\mathbf{H}\mathbf{x_e} + \mathbf{n}, \tag{3.1}$$

where $\mathbf{x_b} = [x_{b_1}, ..., x_{b_{N_t}}]^T \in \mathbb{C}^{N_t \times 1}$ is the transmitted base layer complex vector with $\mathrm{E}[\mathbf{x_b}{\mathbf{x_b}}^H] = E_{x_b}\mathbf{I}$ and $\mathbf{x_e} = [x_{e_1}, ..., x_{e_{N_t}}]^T \in \mathbb{C}^{N_t \times 1}$ is the transmitted enhancement layer complex vector with $\mathrm{E}[\mathbf{x_e}{\mathbf{x_e}}^H] = E_{x_e}\mathbf{I}$. The total transmitted symbol energy equals 1, i.e., $E_{x_b} + E_{x_e} = 1$.

3.1 Receiver Structure

In the proposed receiver, the base layer is detected first with MMSE. The received signal is passed through the MMSE receiver. The filter output is given by

$$\mathbf{z_b} = \mathbf{W^H}\mathbf{y}, \tag{3.2}$$

where $\mathbf{W^H}$ represents MMSE equalization filter. The mean square error (MSE) in the filter output is computed for the base layer vector as

$$J = \mathrm{E}\left[\|\mathbf{z_b} - \mathbf{x_b}\|^2\right]. \tag{3.3}$$

The MMSE filter which minimizes J is found by using (2.11) as follows

$$\begin{aligned}
\mathbf{W^H} &= \mathrm{E}\left[\mathbf{x_b y^H}\right]\left(\mathrm{E}\left[\mathbf{y y^H}\right]\right)^{-1} \\
&= \mathrm{E}\left[\mathbf{x_b}\left(\frac{1}{\sqrt{N_t}}\mathbf{H x_b}+\frac{1}{\sqrt{N_t}}\mathbf{H x_e}+\mathbf{n}\right)^{H}\right] \\
&\quad \left\{\mathrm{E}\left[\left(\frac{1}{\sqrt{N_t}}\mathbf{H x}+\mathbf{n}\right)\left(\frac{1}{\sqrt{N_t}}\mathbf{H x}+\mathbf{n}\right)^{H}\right]\right\}^{-1} \\
&= \mathrm{E}\left[\mathbf{x_b}\left(\frac{1}{\sqrt{N_t}}\mathbf{x_b}^{\mathbf{H}}\mathbf{H^H}+\frac{1}{\sqrt{N_t}}\mathbf{x_e}^{\mathbf{H}}\mathbf{H^H}+\mathbf{n^H}\right)\right] \\
&\quad \left\{\mathrm{E}\left[\left(\frac{1}{\sqrt{N_t}}\mathbf{H x}+\mathbf{n}\right)\left(\frac{1}{\sqrt{N_t}}\mathbf{x^H H^H}+\mathbf{n^H}\right)\right]\right\}^{-1} \\
&= \left(\frac{1}{\sqrt{N_t}}\mathrm{E}\left[\mathbf{x_b}\mathbf{x_b}^{\mathbf{H}}\right]\mathbf{H^H}\right)\left(\frac{1}{N_t}\mathbf{H}\mathrm{E}\left[\mathbf{x x^H}\right]\mathbf{H^H}+\mathrm{E}\left[\mathbf{n n^H}\right]\right)^{-1} \\
&= \frac{E_{x_b}}{\sqrt{N_t}}\mathbf{H^H}\left(\frac{1}{N_t}\mathbf{H H^H}+N_0\mathbf{I}\right)^{-1}. \qquad (3.4)
\end{aligned}$$

Note that the base layer and the enhancement layer signals are uncorrelated since bits of the layers are produced independently, i.e., $\mathrm{E}\left[\mathbf{x_b}\mathbf{x_e}^{\mathbf{H}}\right]=0$ and $\mathrm{E}\left[\mathbf{x_e}\mathbf{x_b}^{\mathbf{H}}\right]=0$.

The MMSE receiver decouples a MIMO system into SISO systems and decisions are made on each filter output $\mathbf{z_b}=[z_{b_1},...,z_{b_{N_t}}]^T$ as

$$\widehat{x}_{b_i}=\underset{\bar{x}_b\in\mathbb{A}_{\mathfrak{X}_\mathfrak{b}}}{\arg\min}\,\|z_{b_i}-\bar{x}_b\|, \qquad (3.5)$$

where $\mathbb{A}_{\mathfrak{X}_\mathfrak{b}}$ is the set of the base layer constellation points. The detected base layer vector is canceled from the received signal by

$$\mathbf{z_e}=y-\frac{1}{\sqrt{N_t}}\mathbf{H}\widehat{\mathbf{x}}_\mathbf{b}, \qquad (3.6)$$

where $\widehat{\mathbf{x}}_\mathbf{b}=[\widehat{x}_{b_1},...,\widehat{x}_{b_{N_t}}]^T$ represents the decoded base layer vector. Finally, the enhancement layer is decoded by joint ML detection as

$$\widehat{\mathbf{x}}_\mathbf{e}=\underset{\bar{\mathbf{x}}_\mathbf{e}\in\mathbb{A}_{\mathfrak{X}_\mathfrak{e}}}{\arg\min}\left\|\mathbf{z_e}-\frac{1}{\sqrt{N_t}}\mathbf{H}\bar{\mathbf{x}}_\mathbf{e}\right\|, \qquad (3.7)$$

where $\mathbb{A}_{\mathfrak{X}_\mathfrak{e}}$ is the set of all possible transmitted $N_t\times 1$ enhancement layer vectors.

The rest of the section presents the receiver structures for the coded and the uncoded cases.

3.1.1 Receiver Structure for the Uncoded Case

Without channel coding in the system, MMSE is used with the SIC method to obtain better performance in the base layer. The enhancement layer of the signal and signals from other antennas are considered as interference. At the MMSE filter output, the base layer with the highest SINR is detected first and canceled from the received signal. A new MMSE filter is designed for the rest of the base layer symbols and this process is repeated until all base layer symbols are detected. Let us assume that the k-th base layer signal has the highest SINR at the MMSE filter output. After detection and assuming perfect cancellation, the rest of the signal vector is written as

$$\tilde{\mathbf{y}} = \frac{1}{\sqrt{N_t}}\tilde{\mathbf{H}}\tilde{\mathbf{x}}_\mathbf{b} + \frac{1}{\sqrt{N_t}}\mathbf{H}\mathbf{x}_\mathbf{e} + \mathbf{n}, \tag{3.8}$$

where $\tilde{\mathbf{H}}$ and $\tilde{\mathbf{x}}_\mathbf{b}$ represented the new channel matrix and the remaining base layer vector that is formed by removing the k-th column of $\mathbf{H}$ and the k-th row of $\mathbf{x_b}$, respectively. The new MMSE filter $\tilde{\mathbf{W}}^\mathbf{H}$ designed for $\tilde{\mathbf{x}}_\mathbf{b}$ vector following the steps explained previously as

$$J = \mathrm{E}\left[\|\tilde{\mathbf{W}}^\mathbf{H}\tilde{\mathbf{y}} - \tilde{\mathbf{x}}_\mathbf{b}\|^2\right] \tag{3.9}$$

$$\begin{aligned}
\tilde{\mathbf{W}}^\mathbf{H} &= \mathrm{E}\left[\tilde{\mathbf{x}}_\mathbf{b}\tilde{\mathbf{y}}^\mathbf{H}\right]\left(\mathrm{E}\left[\tilde{\mathbf{y}}\tilde{\mathbf{y}}^\mathbf{H}\right]\right)^{-1} \\
&= \mathrm{E}\left[\tilde{\mathbf{x}}_\mathbf{b}\left(\frac{1}{\sqrt{N_t}}\tilde{\mathbf{H}}\tilde{\mathbf{x}}_\mathbf{b} + \frac{1}{\sqrt{N_t}}\mathbf{H}\mathbf{x}_\mathbf{e} + \mathbf{n}\right)^H\right] \\
&\quad \left\{\mathrm{E}\left[\left(\frac{1}{\sqrt{N_t}}\tilde{\mathbf{H}}\tilde{\mathbf{x}}_\mathbf{b} + \frac{1}{\sqrt{N_t}}\mathbf{H}\mathbf{x}_\mathbf{e} + \mathbf{n}\right)\left(\frac{1}{\sqrt{N_t}}\tilde{\mathbf{H}}\tilde{\mathbf{x}}_\mathbf{b} + \frac{1}{\sqrt{N_t}}\mathbf{H}\mathbf{x}_\mathbf{e} + \mathbf{n}\right)^H\right]\right\}^{-1} \\
&= \mathrm{E}\left[\tilde{\mathbf{x}}_\mathbf{b}\left(\frac{1}{\sqrt{N_t}}\tilde{\mathbf{x}}_\mathbf{b}^\mathbf{H}\tilde{\mathbf{H}}^\mathbf{H} + \frac{1}{\sqrt{N_t}}\mathbf{x_e}^\mathbf{H}\mathbf{H}^\mathbf{H} + \mathbf{n}^\mathbf{H}\right)\right] \\
&\quad \left\{\mathrm{E}\left[\left(\frac{1}{\sqrt{N_t}}\tilde{\mathbf{H}}\tilde{\mathbf{x}}_\mathbf{b} + \frac{1}{\sqrt{N_t}}\mathbf{H}\mathbf{x}_\mathbf{e} + \mathbf{n}\right)\left(\frac{1}{\sqrt{N_t}}\tilde{\mathbf{x}}_\mathbf{b}^\mathbf{H}\tilde{\mathbf{H}}^\mathbf{H} + \frac{1}{\sqrt{N_t}}\mathbf{x_e}^\mathbf{H}\mathbf{H}^\mathbf{H} + \mathbf{n}^\mathbf{H}\right)\right]\right\}^{-1} \\
&= \left(\frac{1}{\sqrt{N_t}}\mathrm{E}\left[\tilde{\mathbf{x}}_\mathbf{b}\tilde{\mathbf{x}}_\mathbf{b}^\mathbf{H}\right]\tilde{\mathbf{H}}^\mathbf{H}\right) \\
&\quad \left(\frac{1}{N_t}\tilde{\mathbf{H}}\mathrm{E}\left[\tilde{\mathbf{x}}_\mathbf{b}\tilde{\mathbf{x}}_\mathbf{b}^\mathbf{H}\right]\tilde{\mathbf{H}}^\mathbf{H} + \frac{1}{N_t}\mathbf{H}\mathrm{E}\left[\mathbf{x_e}\mathbf{x_e}^\mathbf{H}\right]\mathbf{H}^\mathbf{H} + \mathrm{E}\left[\mathbf{n}\mathbf{n}^\mathbf{H}\right]\right)^{-1} \\
&= \frac{E_{x_b}}{\sqrt{N_t}}\tilde{\mathbf{H}}^\mathbf{H}\left(\frac{E_{x_b}}{N_t}\tilde{\mathbf{H}}\tilde{\mathbf{H}}^\mathbf{H} + \frac{E_{x_e}}{N_t}\mathbf{H}\mathbf{H}^\mathbf{H} + N_0\mathbf{I}\right)^{-1}.
\end{aligned} \tag{3.10}$$

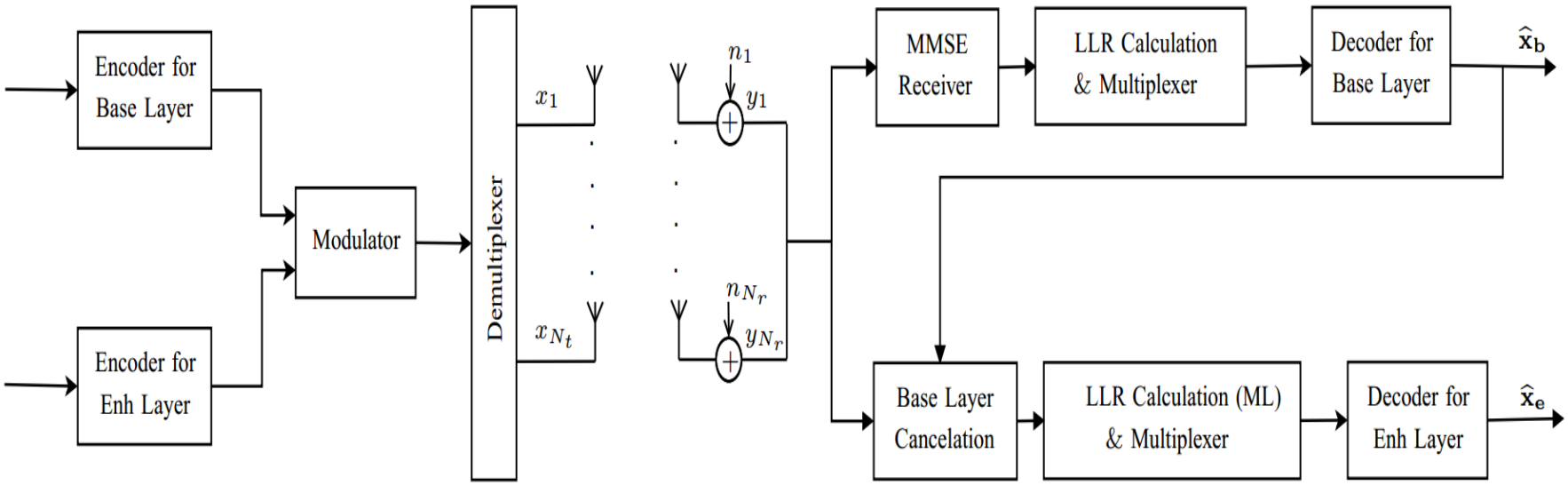

Figure 3.2: Coded System Structure

3.1.2 Receiver Structure for the Coded Case

The SIC method isn't used in the coded system to keep receiver structure simpler since the base layer has a much better performance with coding compared to the uncoded case. Otherwise, encoding should be done N_t times for the cancellation operations of the SIC in the base layer. Figure 3.2 shows system structure. As it is seen in the figure, two encoders are used for each layer in our system, therefore, hard detection of the base layer can be performed. The Hermitian transpose of the MMSE filter in (3.4) is written as

$$\mathbf{W} = \begin{bmatrix} | & | & & | \\ \mathbf{g_1} & \mathbf{g_2} & \cdots & \mathbf{g_{N_t}} \\ | & | & & | \end{bmatrix} \tag{3.11}$$

where $\mathbf{g_i}$ is the filter vector which produces the i-th output of the MMSE filter. The filter vector is represented as

$$\mathbf{g_i} = \frac{E_{x_b}}{\sqrt{N_t}} \left(\frac{1}{N_t} \mathbf{H}\mathbf{H^H} + N_0 \mathbf{I} \right)^{-1} \mathbf{h_i}. \tag{3.12}$$

Passing the received vector through the filter vectors yields

$$z_{bi} = \mathbf{g_i^H y} = \beta_i x_{bi} + \eta_i, \tag{3.13}$$

where β_i is the desired signal term

$$\beta_i = \frac{1}{\sqrt{N_t}} \mathbf{g_i^H h_i} \tag{3.14}$$

and η_i is the interference-plus-noise term modeled as a complex Gaussian random variable given by

$$\eta_i = \frac{1}{\sqrt{N_t}} \mathbf{g_i^H h_i} x_{ei} + \sum_{k \neq i} \frac{1}{\sqrt{N_t}} \mathbf{g_i^H h_k} x_k + \mathbf{g_i^H n}. \tag{3.15}$$

From the i-th MMSE receiver output, the log likelihood ratio corresponding the j-th base layer bit of the i-th input antenna is calculated as

$$\begin{aligned} \Lambda_b(b^{j,i}|z_i, \beta_i, {\sigma_{\eta_i}}^2) &= \ln \frac{\Pr(b^{j,i} = 1 | z_{b_i}, \beta_i, {\sigma_{\eta_i}}^2)}{\Pr(b^{j,i} = 0 | z_{b_i}, \beta_i, {\sigma_{\eta_i}}^2)} \\ &= \ln \frac{\sum_{\tilde{x}_b \in B_1^j} \Pr(z_{b_i} \mid \tilde{x}_b, \beta_i, {\sigma_{\eta_i}}^2)}{\sum_{\tilde{x}_b \in B_0^j} \Pr(z_{b_i} \mid \tilde{x}_b, \beta_i, {\sigma_{\eta_i}}^2)} \\ &= \ln \frac{\sum_{\tilde{x}_b \in B_1^j} \exp\left(-\frac{|z_{bi} - \beta_i \tilde{x}_b|^2}{{\sigma_{\eta_i}}^2} \right)}{\sum_{\tilde{x}_b \in B_0^j} \exp\left(-\frac{|z_{bi} - \beta_i \tilde{x}_b|^2}{{\sigma_{\eta_i}}^2} \right)}, \end{aligned} \tag{3.16}$$

where B_1^j and B_0^j are the the subsets of the base layer constellation points with j-th bit equal to 1 and 0, respectively and ${\sigma_{\eta_i}}^2$ is the variance of η_i.

After LLR's for the base layer are determined and passed into the base layer decoder, hard decisions are made for the base layer symbols. Cancellation of the base layer is performed based on these hard decisions and the vector $\mathbf{z_e}$ is obtained. The log-likelihood ratios based on the ML receiver corresponding the j-th enhancement layer bit transmitted from the i-th antenna is calculated as

$$\begin{aligned}\Lambda_e(b^{j,i}|\mathbf{z_e},\mathbf{H}) &= \ln\frac{\Pr(b^{j,i}=1|\mathbf{z_e},\mathbf{H})}{\Pr(b^{j,i}=0|\mathbf{z_e},\mathbf{H})} \\ &= \ln\frac{\sum_{\tilde{\mathbf{x}}_\mathbf{e}\in E_1^{j,i}}\Pr(\mathbf{z_e}\mid\tilde{\mathbf{x}}_\mathbf{e},\mathbf{H})}{\sum_{\tilde{\mathbf{x}}_\mathbf{e}\in E_0^{j,i}}\Pr(\mathbf{z_e}\mid\tilde{\mathbf{x}}_\mathbf{e},\mathbf{H})} \\ &= \ln\frac{\sum_{\tilde{\mathbf{x}}_\mathbf{e}\in E_1^{j,i}}\exp\left(-\frac{\left\|\mathbf{z_e}-\frac{1}{\sqrt{N_t}}\mathbf{H}\tilde{\mathbf{x}}_\mathbf{e}\right\|^2}{N_0}\right)}{\sum_{\tilde{\mathbf{x}}_\mathbf{e}\in E_0^{j,i}}\exp\left(-\frac{\left\|\mathbf{z_e}-\frac{1}{\sqrt{N_t}}\mathbf{H}\tilde{\mathbf{x}}_\mathbf{e}\right\|^2}{N_0}\right)},\end{aligned} \tag{3.17}$$

where $E_1^{j,i}$ and $E_0^{j,i}$ are the the subsets of the enhancement layer constellation transmitted from the i-th antenna with j-th bit equal to 1 and 0, respectively. It is assumed that all bits are equally likely to be transmitted in each layer.

As it is observed in (3.17), the ML receiver [18]- [19] we refer to in this work is an ML demodulator, rather than a full sequence detector. The optimum ML receiver would perform decoding and demodulation jointly. However, it is too unpractical since the computational complexity of the optimum ML receiver is enormous. Note that even the ML demodulator used in our work has a high computational complexity and hence we aim avoiding it by the scheme proposed in this work.

3.2 Computational Complexity Analysis

The computational complexity can be considered as the sum of the preparation complexity and the vector processing complexity.

- The preparation complexity corresponds to one-time-only operations, in other words, the operations are performed once within a block that the channel matrix

does not change.

- The vector processing complexity comprises the operations which are repeated for each received vector. All received vectors are processed one by one.

Let us consider the case where the number of transmitter and receiver antennas are equal, i.e., $N_r = N_t = N$. Assuming block length L is much greater than N, the overall complexity tends to be dominated by vector processing complexity. The orders of overall computational complexities per received vector within a block are derived for the receiver structures in this section. We consider multiplication operations in computational complexity calculations.

3.2.1 Computational Complexity for the Uncoded Case

ML detection is the optimum receiver structure. Reminding (2.5), ML detection is a brute-force search over the set $\mathbb{A}_{\mathfrak{X}}$. The set $\mathbb{A}_{\mathfrak{X}}$ has size of M^N. The computational complexity of ML receiver grows exponentially with the number of transmit antennas. Let us examine ML complexity a little deeper:

- The preparation complexity corresponds to calculating $\mathbf{H}\bar{\mathbf{x}}$ for all the possible transmitted codewords with complexity $\mathcal{O}(M^N N^2)$. Note that matrix multiplication $\mathbf{H}\bar{\mathbf{x}}$ has complexity $\mathcal{O}(N^2)$.
- The vector processing complexity equals $\mathcal{O}(NLM^N)$ since the norm operation is performed LM^N times. Note that one norm operation have complexity $\mathcal{O}(N)$.
- The overall complexity can be written as $\mathcal{O}(M^N N^2 + NLM^N) \approx \mathcal{O}(NLM^N)$ by $L >> N$.

Hence, the computational complexity per received vector in the ML receiver is $\mathcal{O}(NM^N)$.

Let us examine the computational complexity of the MMSE-SIC receiver structure:

- The computational complexity of calculating an MMSE filter matrix is $\mathcal{O}(N^3)$.

In the SIC method, N filters are used, therefore, the preparation complexity of MMSE-SIC receiver is $\mathcal{O}(N^4)$.

- The bulk of vector processing complexity is the equalization step. One equalization operation has complexity $\mathcal{O}(N^2)$. Due to SIC, N equalizations are performed per received vector and NL is the total number of equalizations within a block.
- The overall complexity can be written as $\mathcal{O}(N^4 + LN^3) \approx \mathcal{O}(LN^3)$ since $L >> N$.

Finally, the computational complexity per received vector of MMSE-SIC receiver is $\mathcal{O}(N^3)$.

By combining the computational complexities of the ML and the MMSE-SIC receivers, the computational complexity per received vector of the proposed receiver structure can be calculated as:

- First, the base layer is detected with MMSE-SIC receiver. Computational complexity of the base layer is $\mathcal{O}(N^3)$.
- It is followed by the enhancement layer with ML detection. Exhaustive search is performed over the set with size 4^N since 4-QAM is transmitted in the enhancement layer. Therefore, computational complexity of the enhancement layer is $\mathcal{O}(N4^N)$.
- As a conclusion, the overall computational complexity of the proposed receiver is $\mathcal{O}(N^3) + \mathcal{O}(N4^N)$. For the systems with a high number of antennas, the proposed receiver's computational complexity is approximately $\mathcal{O}(N4^N)$.

If data was transmitted with 16-QAM modulation that has the same data rate with 16-HQAM, complexity would be $\mathcal{O}(N16^N)$ in the case of optimum ML detection. Complexity can be decreased to $\mathcal{O}(N^3)$ with MMSE-SIC receiver. However, significant performance losses can be suffered in comparison with ML. In the proposed receiver, the receiver complexity is approximately $\mathcal{O}(N4^N)$, which is significantly less than the complexity of ML receiver. Table 3.1 shows a comparison of computational complexities of receivers for the uncoded case.

3.2.2 Computational Complexity for the Coded Case

In a coded system, MMSE is used without SIC method to keep receiver structure simpler. In the complexity calculations, LDPC decoding complexities are not considered since decoding complexities are equal for all receiver structures.

- Computational complexity per received vector in the ML case is $\mathcal{O}(NM^N)$ due to the number of operation are required to evaluate the norms appering in (3.17).
- MMSE receiver decomposes the MIMO system into multiple SISO systems, therefore LLR calculations depend only the constellation points. Therefore, the bulk of complexity for MMSE receiver is in computing $\mathbf{W}$ and equalization. Since a single MMSE filter is used, the preparation complexity is $\mathcal{O}(N^3)$. The vector processing complexity is equal to $\mathcal{O}(LN^2)$, since a single equalization operation is performed per received vector and L is the total number of equalizations within a block. Hence, the overall computational complexity per received vector of the MMSE case is $\mathcal{O}(N^2)$.
- The overall complexity of the structure proposed here is $\mathcal{O}(N^2) + \mathcal{O}(N4^N)$.

Table 3.2 shows a comparison of computational complexities of receivers for the coded case.

Table3.1: Computational Complexities of the Uncoded Case

	Complexity
16-QAM ML Receiver	$\mathcal{O}(N16^N)$
16-QAM MMSE-SIC Receiver	$\mathcal{O}(N^3)$
The Proposed Receiver	$\mathcal{O}(N^3) + \mathcal{O}(N4^N)$

Table3.2: Computational Complexities of the Coded Case

	Complexity
16-QAM ML Receiver	$\mathcal{O}(N16^N)$
16-QAM MMSE-SIC Receiver	$\mathcal{O}(N^2)$
The Proposed Receiver	$\mathcal{O}(N^2) + \mathcal{O}(N4^N)$

CHAPTER 4

RESULTS

Uncoded and coded system performances are presented for 2×2 and 4×4 cases in this chapter. Furthermore, performances of different receiver structures, that are alternative to the proposed one, are compared.

4.1 The Uncoded Case

MMSE receiver always has diversity $N_r - N_t + 1$ in an uncoded MIMO system. Therefore, the base layer has a diversity order of 1 in our case $N_r = N_t$. This can be observed in figures for uncoded transmission where diversity order increase cannot be attained in the base layer due to MMSE detection. Base layer error curves' slopes are equal to 1. For the $N_r \times N_t$ MIMO uncoded system, one expects to observe a diversity order of N_r in the ML receiver, but in Figure 4.1 the enhancement layer does not reach that limit. If the receiver had a perfect base layer knowledge for a 2×2 system, the expected diversity order of 2 is observed at the enhancement layer in Figure 4.1. Base layer errors propagate to the enhancement layer so that BER performance of the enhancement layer is limited by the BER performance of the base layer.

Figure 4.2 shows a 2×2 uncoded system's BER performance for ML, MMSE-SIC and the proposed receiver structures. Performances of the base and enhancement layers, and the the average performance of the layers are presented in the figure. As it is observed, the average performance is closer to the enhancement layer. This is due to fact that the y-axis has a logarithmic scale and thus average is closer the worse

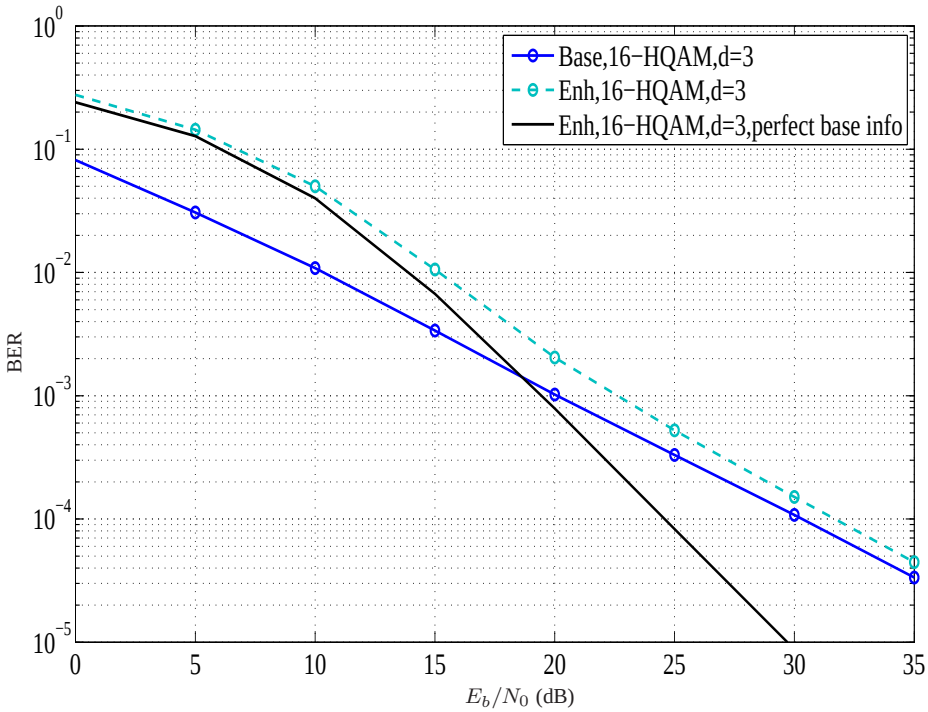

Figure 4.1: BER for uncoded 2×2 MIMO system with perfect base layer information

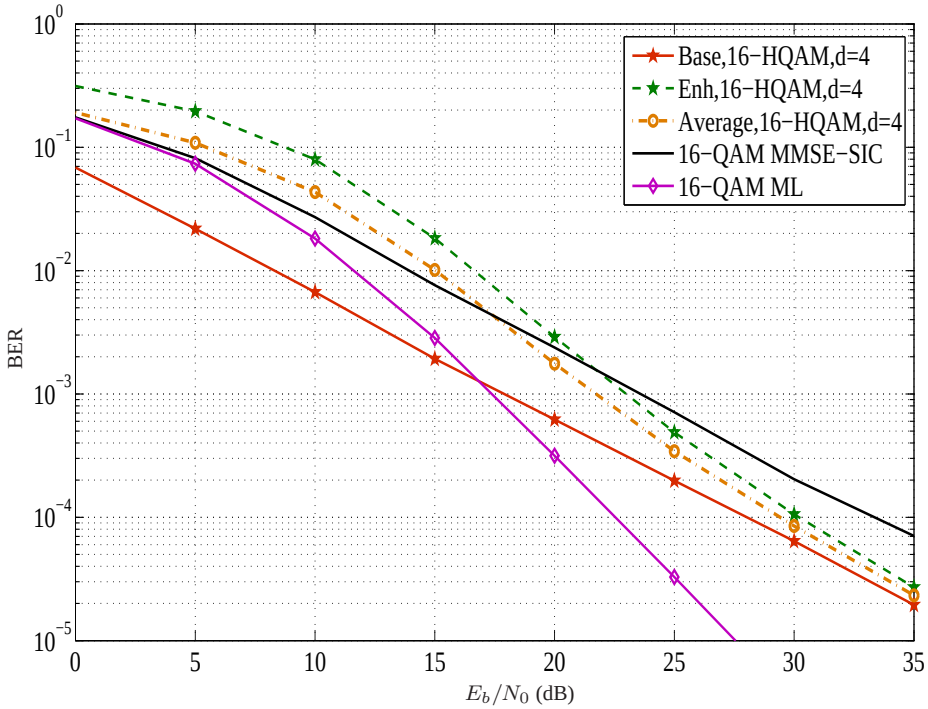

Figure 4.2: BER for uncoded 2×2 MIMO system

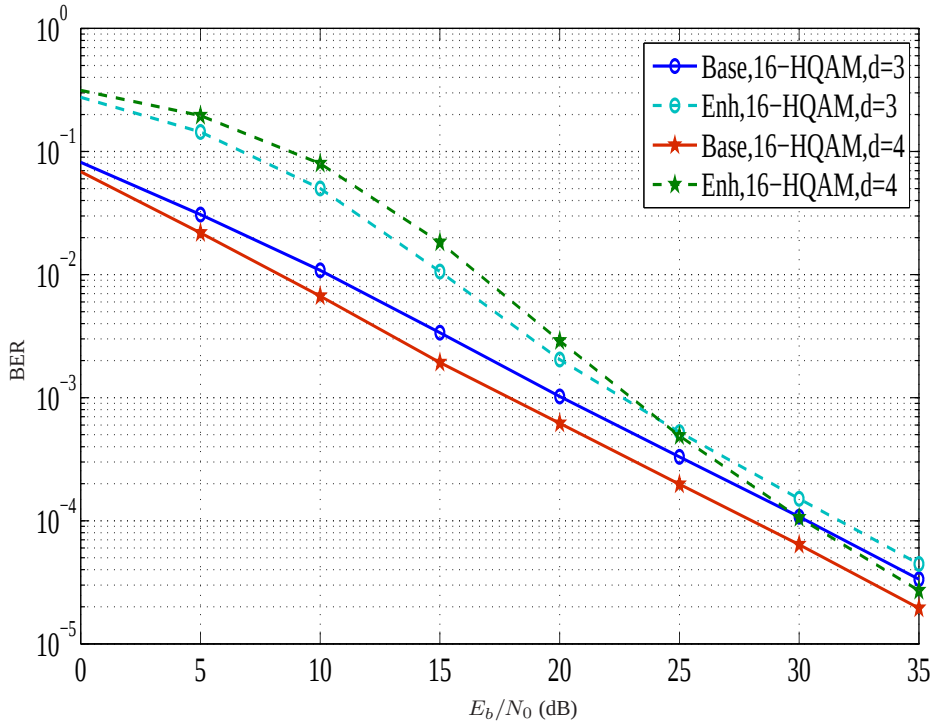

Figure 4.3: The proposed receiver BER for uncoded 2×2 MIMO system with different d ratios

error curve.

Note that in some of the figures, the average performance is not provided not to overcrowd the graphs. In such a case, one may envision that the average performance is closer to that of the enhancement layer.

In Figure 4.2, there is approximately 11 dB performance gap between ML and MMSE-SIC receivers at $\mathrm{BER} = 10^{-4}$. On the other hand, the performance gap between ML and the proposed receiver with $d = 4$ is approximately 7 dB.

Figure 4.3 shows a 2×2 uncoded system's BER performance of the proposed receiver structures for different d ratios. The base layer has better performance with higher d due to a higher protection level of the base layer and thus reduced error propagation. Hence, enhancement layer performance for the case $d = 4$ has higher error rate at low SNRs, since it is less protected. However, the behavior changes at high SNRs due to lower error level limited by the base layer. At the 10^{-4} BER target, the average system performance for $d = 4$ is around 1.5 dB better than the performance for $d = 3$.

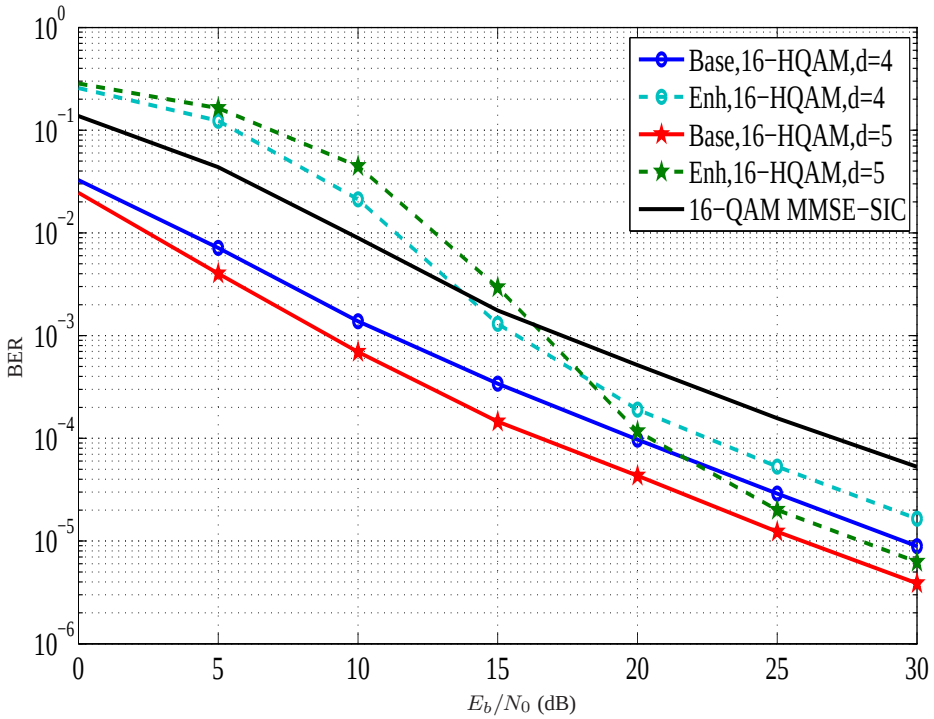

Figure 4.4: BER for uncoded 4×4 MIMO system

Figure 4.4 shows a 4×4 uncoded system's BER performance. The proposed structure performs better than MMSE-SIC, approximately 6 dB with $d = 4$ and 7.5 dB with $d = 5$ at $\mathrm{BER} = 10^{-4}$. Figure 4.3 and Figure 4.4 verifies that when d increases, the base layer has better BER performance and the enhancement layer has worse BER performance at low SNRs since enhancement layer symbols have smaller energy for larger d values. When SNR increases, BER performances of both layers come closer and enhancement layer BER is limited by the base layer once more due to error propagation. It is also observed that d does not affect the diversity order.

4.1.1 Alternative Receiver Structures

Using different receiver structures at different layers can be considered. Figure 4.5 shows BER performance of detecting both layers sequentially by ML receivers. Error floor surfaces due to the interference of the enhancement layer to the base layer. The level of error floor is lower for the case of $d = 8$, because the interference on the base layer is decreased by sending the enhancement layer at a lower energy. In the

proposed receiver structure, the interference is minimized by the MMSE receiver which helps the proposed structure operate well. The system has a lower overall interference after MMSE based base layer detection. After base layer detection, the base layer ideally has no interference influencing on the enhancement layer so that enhancement layer can be smoothly detected with ML.

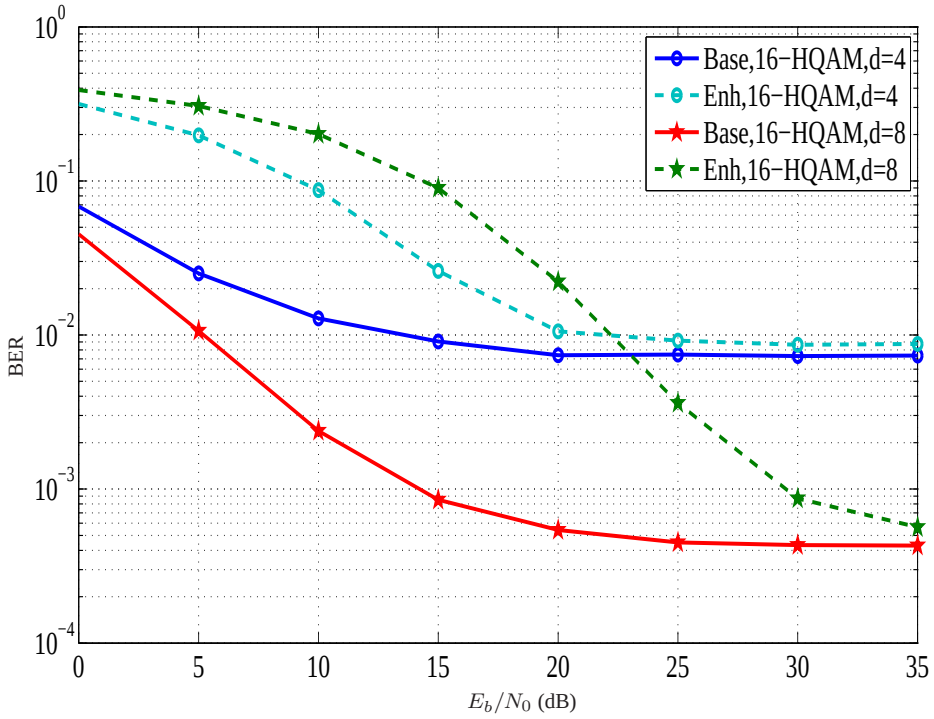

Figure 4.5: BER for uncoded 2×2 MIMO system, operate on both layers ML

Using MMSE receiver in the enhancement layer also can be considered. MMSE receiver for the base layer can be designed as

$$\mathbf{W^H} = \frac{E_{x_e}}{\sqrt{N_t}}\mathbf{H^H}\left(\frac{E_{x_e}}{N_t}\mathbf{HH^H} + N_0\mathbf{I}\right)^{-1}.$$

Since we know MMSE receiver in base layer minimizes the interference, ML receiver is preferred due to its better performance. If MMSE was used in enhancement layer, the performance would be like in Figure 4.6. As it is expected, MMSE has performance lose compared to ML.

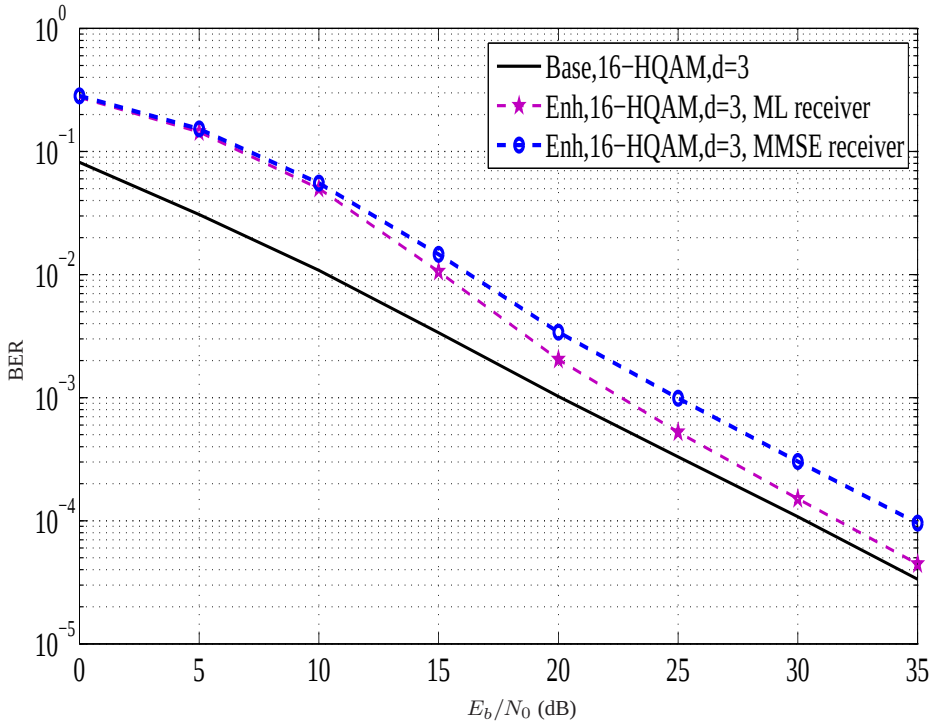

Figure 4.6: BER for uncoded 2×2 MIMO system, operate on both layers MMSE

4.2 The Coded Case

WiMAX LDPC codes defined in the IEEE 802.16e standard are used in our study. Detailed information can be found in Appendix A and the mentioned standard [20]. The frame length is fixed at 2304 in this work, which is the largest code length of WiMAX LDPC codes. A sequence of 2304 bits are generated at the output of the encoder for standard 16-QAM and 1152 bits are generated at the output of each layer's encoder for 16-HQAM. The number of maximum iterations are set to 50 in the LDPC decoder. Decoding operation stops when early termination detected. Each frame is transmitted over $F = 8$ blocks that have independent and identically distributed fading. The code rates of the base layer and the enhancement layer are expressed as R_b and R_e, respectively. The overall code rate is defined by

$$R = \frac{R_b + R_e}{2}.$$

A high spectral efficiency is desired in the system, therefore an overall system code rate of $R = 3/4$ is chosen. Frame error rate (FER) performances are examined.

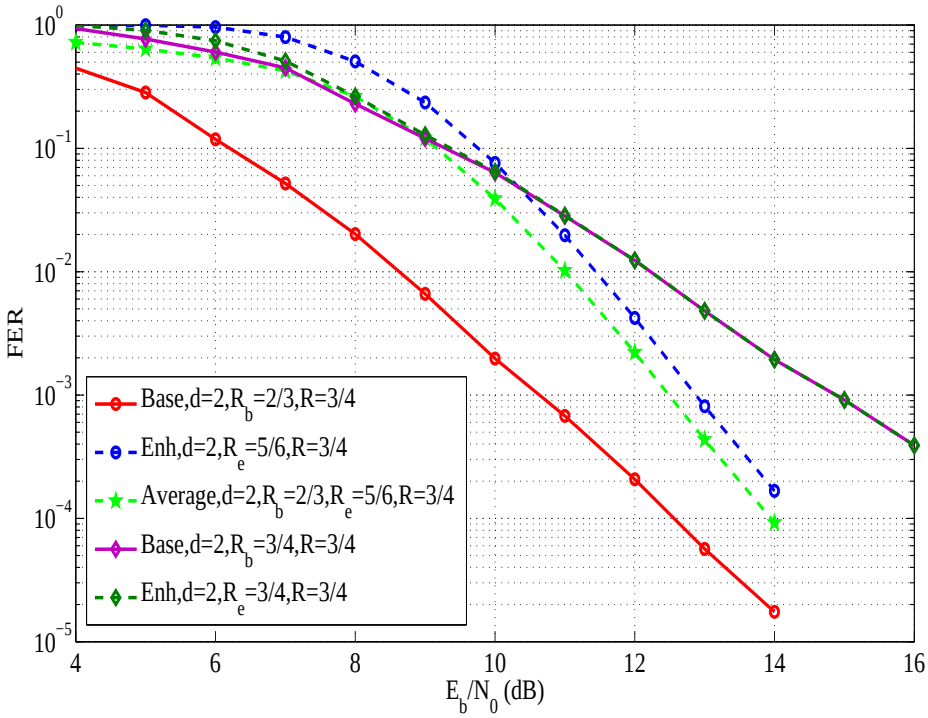

Figure 4.7: FER for coded 2×2 MIMO system with fixed $d = 2$, F=8

As it is observed in Figure 4.7, average performance is much closer to the enhancement layer performance. It can be said that total system performance is dominated by the enhancement layer. Unless the UEP property of hierarchical modulation is the goal of the system, having large performance gap between layers may not a desired feature. Performance of layers can be adjusted by changing either d like we did in the uncoded case or code rates of the layers.

In the Figure 4.7, the constellation ratio d of 16-HQAM is fixed to 2 and the effect of code rates are examined. The performance gap between layers is higher when $R_b = 2/3$ and $R_e = 5/6$. Using the same code rate in both layers ($R_b = R_e = 3/4$) brings the performances of layers closer yet at the cost of worse FER. The effect of code rates on the performance can be analyzed by considering the Singleton diversity bound for block fading SISO systems [21]

$$\text{diversity} \leq \lfloor F(1-R) \rfloor + 1.$$

Increasing R_b from $2/3$ to $3/4$ results in poor diversity order in the base layer. Decreasing R_e from $5/6$ to $3/4$ may be expected to lead to a higher diversity order in the

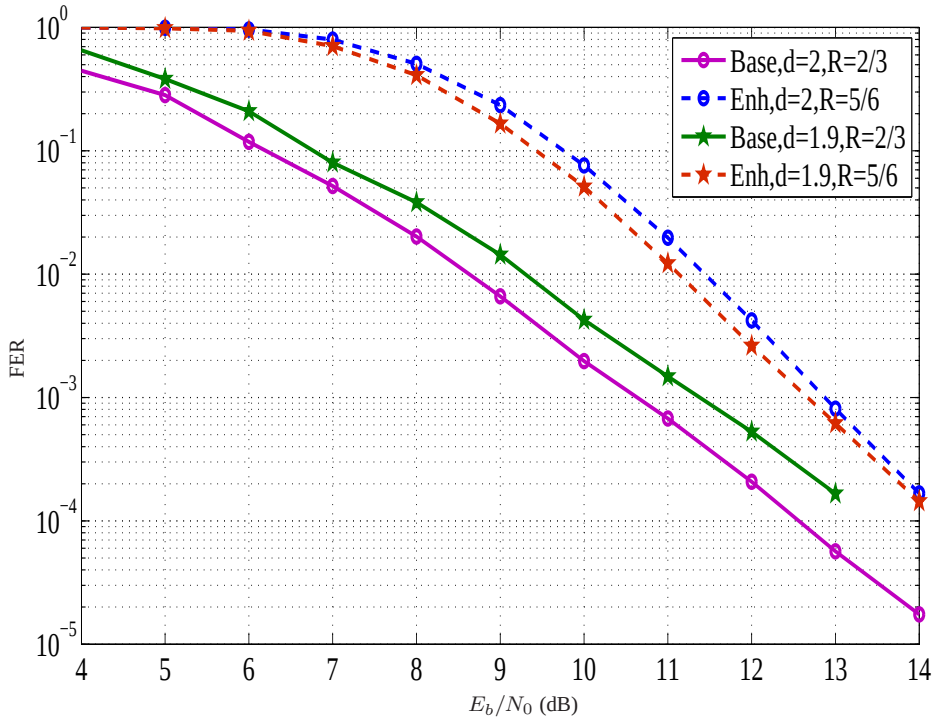

Figure 4.8: FER for coded 2×2 MIMO system with fixed $R_b = 2/3$ and $R_e = 5/6$, F=8

enhancement layer, which is immaterial since the enhancement layer performance is limited by that of the base layer. Due to the fact that MMSE receiver lacks spatial diversity, using lower code rates in the base layer is appropriate to obtain frequency diversity. In the enhancement layer, higher code rates are used to keep the overall code rate constant.

Alternatively, rather than changing code rates, varying d may be more proper to adjust the performance gap between layers. In Figure 4.8, code rates are fixed to $R_b = 2/3$ and $R_e = 5/6$ and the effect of d is examined. When d decreases, performances of both layers come closer as also observed for the uncoded case.

Figure 4.9 shows a 2×2 coded system's FER performance of ML with $R = 3/4$, of MMSE with $R = 3/4$ and of the proposed receiver structure with $d = 1.9$, $R_b = 2/3$ and $R_e = 5/6$. For $\mathrm{FER} = 10^{-3}$, the proposed structure performs around 0.5 dB off from the ML. Moreover, the proposed structure shows around 4.5 dB better performance than the MMSE. The average performance of the coded proposed structure is

much closer to ML relative to the uncoded case. This seems from the fact that MMSE receiver has better diversity order in the coded case.

Figure 4.10 shows a 4×4 coded system's FER performance of MMSE and the proposed receiver structures with $d = 2$, $R_b = 2/3$ and $R_e = 5/6$ where ML detector performance is not depicted since statistically significant numerical results were not available due to the very high running time of the ML detector. For $\mathrm{FER} = 10^{-3}$, the proposed receiver has approximately 6.5 dB SNR advantage when compared to MMSE receiver.

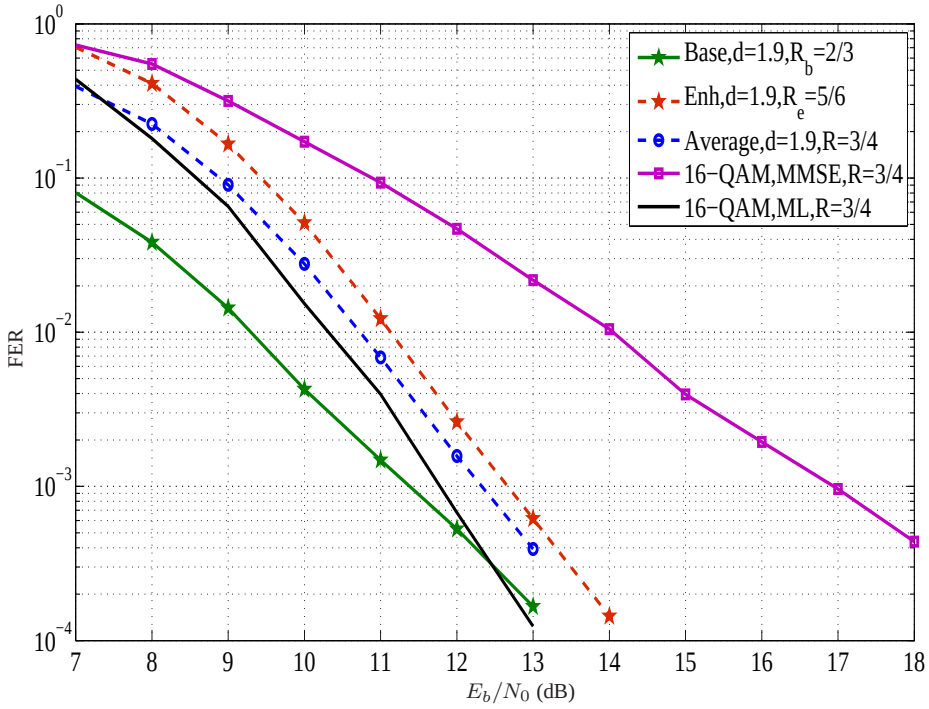

Figure 4.9: FER for coded 2×2 MIMO system

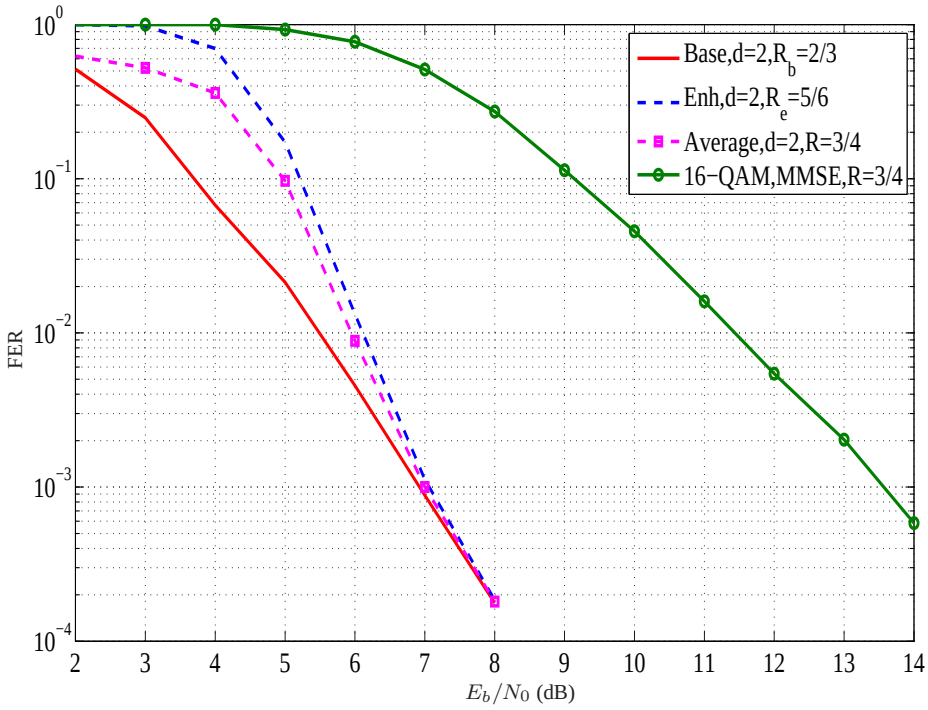

Figure 4.10: FER for coded 4×4 MIMO system

CHAPTER 5

CONCLUSIONS

In this work, a new receiver structure with low computational complexity is proposed for MIMO systems. The idea makes use of hierarchical modulation so that processing is performed sequentially for each layer. The proposed scheme provides a performance between that of ML receiver and MMSE-SIC receiver at a significant lower complexity. With carefully chosen parameters and coding rates, performance quite close to that of ML receiver can be achieved in settings of practical interest.

For the uncoded case, MMSE is used with the SIC method in the base layer in order to have a better performance. By optimizing d ratios, significant error rate performance improvements are provided in comparison with the MMSE-SIC receiver. However, the proposed receiver structure's performance is still far away from that of ML. This is due to the fact that MMSE cannot attain space diversity, therefore, it causes a poor performance in the base layer as well as in the enhancement layer becasue of the error propogation.

For the coded case, SIC is not utilized in order to keep the system structure simpler. MMSE filtering without the SIC method works well with the block fading model since MMSE in the base layer starts to achieve diversity. Flexibility of hierarchical modulation is utilized in the system, e.g., through different code rates in layers and changing the constellation ratio d. Using different code rates in layers provides opportunity to have a system with higher spectral efficiency. This seems from the fact that better base layer performance results in better enhancement layer performance as SNR increases since error propagation is avoided. Error performances of the layers can be kept close to each other by adjusting d ratios. By properly choosing the d ra-

tios, considerable error rate performance improvements are observed in comparison with that of MMSE receiver. It is observed that the proposed structure can sometimes achieve near ML performance. The proposed receiver performs around 0.5 dB off from the ML performance with optimized d and R parameters at $\mathrm{FER} = 10^{-3}$ for a 2×2 system transmitted over 8 fading blocks.

Furthermore, receiver computational complexity drops from $\mathcal{O}(N16^N)$ to $\mathcal{O}(N4^N)$ when compared with that of ML for the number of transmitter and receiver antennas are equal, i.e., $N_r = N_t = N$. The proposed structure has significant complexity advantage, especially for MIMO systems with a high number of antennas.

Future Work:

In this work, SIC is not used in the coded case to keep the system simpler. However, as an extension of this work low complexity architectures with SIC may be investigated.

A two-stage receiver is considered for 16-QAM hierarchical modulation. Systems with higher data rates can be examined as a future work, e.g., a three-stage receiver for 64-QAM hierarchical modulation. This future work can focus on designing parameters like choosing d ratios of 64-HQAM constellation, finding correct coding rates of three layers and using proper receiver types in each layer.

The basic idea and the design presented in this work can be extended and/or modified to be utilized in massive MIMO (very large MIMO) implementations for next generation wireless systems.

REFERENCES

[1] I. E. Telatar, “Capacity of multi-antenna Gaussian channels," *European Transactions on Telecommunications*, vol. 10, pp. 585-595, November/December 1999.

[2] G. J. Foschini, “Layered space-time architecture for wireless communication in a fading environment when using multiple antennas," *Bell Labs Technical Journal*, vol. 1, no. 2, pp. 41-59, Autumn 1996.

[3] P. W. Wolniansky, G. J. Foschini, G. D. Golden, and R. A. Valenzuela, “V-BLAST: An architecture for realizing very high data rates over the rich-scattering wireless channel,” *URSI International Symposium on Signals, Systems, and Electronics (ISSSE)*, September 1998, pp. 295–300.

[4] U. Fincke and M. Pohst, “Improved methods for calculating vectors of short length in a lattice, including a complexity analysis,” *Mathematics of Computation*, vol. 44, pp. 463–471, April 1985.

[5] J. Jalden and B. Ottersten, “On the complexity of sphere decoding in digital communications," *IEEE Transactions on Signal Processing*, vol. 53, no. 4, pp. 1474-1484, April 2005.

[6] T. Cover, “Broadcast channels," *IEEE Transactions on Information Theory*, vol. IT-18, no. 1, pp. 2-14, January 1972.

[7] *Digital Video Broadcasting (DVB); framing structure, channel coding and modulation for digital terrestrial television*, ETSI EN 300 744 V1.5.1, 2004.

[8] H. Jiang and P. A. Wilford, “A hierarchical modulation for upgrading digital broadcast systems," *IEEE Transactions on Broadcasting*, vol. 51, no. 2, pp. 223-229, June 2005.

[9] M. Rupp, G. Gritsch and H. Weinrichter, “Approximate ML detection for MIMO systems with very low complexity," *IEEE International Conference on Acoustics, Speech, and Signal Processing (ICASSP)*, May 2004, pp. 809-812.

[10] A. Sibille, C. Oestges and A. Zanella. *MIMO from theory to implementation.* Academic Press, 2010.

[11] K. B. Petersen and M. S. Pedersen. (2012, November 15). *The matrix cookbook* [Online]. Available: http://matrixcookbook.com

[12] P. K. Vitthaladevuni and M.-S. Alouini, “BER Computation of $4/M$-QAM hierarchical constellations," *IEEE Transactions on Broadcasting*, vol. 47, no. 3, pp. 228-239, September 2001.

[13] E. Biglieri, J. Proakis and S. Shamai, “Fading channels: information-theoretic and communications aspects," *IEEE Transactions on Information Theory*, vol. 44, no. 6, pp. 2619-2692, October 1998.

[14] A. Hedayat and A. Nosratinia, "Outage and diversity of linear receivers in flat-fading MIMO channels," *IEEE Transactions on Signal Processing*, vol. 55, no. 12, pp. 5868-5873, December 2007.

[15] R. Knopp and P. A. Humblet, “On coding for block fading channels," *IEEE Transactions on Communications*, vol. 46, no. 1, pp. 189-205, January 2000.

[16] R. G. Gallager, “Low-density parity-check codes," *IRE Transactions on Information Theory*, vol. IT-8, pp. 21-28, January 1962.

[17] D. J. C. MacKay and R. M. Neal, “Near Shannon limit performance of low density parity check codes," *IEEE Electronics Letters*, vol. 32, no. 18, pp. 1645-1646, August 1996.

[18] M. R. McKay and I. B. Collings, “Capacity and performance of MIMO-BICM with zero-forcing receivers," *IEEE Transactions on Communications*, vol. 53, no. 1, pp. 74-83, January 2005.

[19] M. R. G. Butler and I. B. Collings, “A zero-forcing approximate log-likelihood receiver for MIMO bit-interleaved coded modulation," *IEEE Communications Letters*, vol. 8, no. 2, pp. 105-107, February 2004.

[20] *IEEE Standard for Local and metropolitan area networks Part 16: Air Interface for Broadband Wireless Access Systems*, IEEE Std 802.16, 2009.

[21] E. Malkamaki and H. Leib, “Coded diversity on block-fading channels," *IEEE Transactions on Information Theory*, vol. 45, no. 2, pp. 771-781, March 1999.

APPENDIX A

WIMAX LDPC CODES

WiMAX LDPC codes are preferred to be used due to proper code lengths and code rates for this work. It supports 4 different code rates $1/2$, $2/3$, $3/4$ and $5/6$ with 19 distinct codeword sizes ranging from 576 bits to 2304 bits. LDPC code can be represented (n, k) and codeword lengths can be chosen according:

$$n = 576 + 96f, \quad 0 \leq f \leq 18 \tag{A.1}$$

then k is chosen according to code rate as

$$k = Rn. \tag{A.2}$$

The parity check matrix $\mathbf{P}$ of size $(n - k) \times n$ can be created from 6 fundamental matrices $1/2$, $2/3$ A, $2/3$ B, $3/4$ A, $3/4$ B and $5/6$. The parity check matrix $\mathbf{P}$ is expanded from a base matrix $\mathbf{P_b}$ of size $m_b \times n_b$. The values of m_b is chosen acording to

$$m_b = (n - k)/z_f \tag{A.3}$$

and n_b has the constant value of 24 and has this relation

$$n_b = n/z_f, \tag{A.4}$$

where z_f is the expansion factor. There are 19 expansion factors taking values according to

$$z_f = n/24 = 24 + 4f, \quad 0 \leq f \leq 18. \tag{A.5}$$

The parity check matrix $\mathbf{P}$ is defined as

$$\mathbf{H} = \begin{bmatrix} \mathbf{P_{1,1}} & \mathbf{P_{1,2}} & \dots & \mathbf{P_{1,n_b}} \\ \mathbf{P_{2,1}} & \mathbf{P_{2,2}} & \dots & \mathbf{P_{2,n_b}} \\ \vdots & \vdots & \vdots & \vdots \\ \vdots & \vdots & \vdots & \vdots \\ \mathbf{P_{m_b,1}} & \mathbf{P_{m_b,2}} & \dots & \mathbf{P_{m_b,n_b}} \end{bmatrix}.$$

where $\mathbf{P_{i,j}}$ is a $z_f \times z_f$ matrix. It can be a null matrix or a identity matrix circularly right-shifted according to the shift value $p(f, i_f, i_r)$. The shift values are derived from $p(i_f, i_r)$, which is the original shift values in base matrices.

For code rates $1/2$, $2/3B$, $3/4A$, $3/4B$ and $5/6$, the shift values corresponding to expansion factor is found as

$$p(f, i_f, i_r) = \begin{cases} p(i_f, i_r) & p(i_f, i_r) \leq 0 \\ \left\lfloor \frac{p(i_f, i_r) z_f}{96} \right\rfloor & p(i_f, i_r) > 0 \end{cases} \tag{A.6}$$

and similarly, for code rates $2/3A$

$$p(f, i_f, i_r) = \begin{cases} p(i_f, i_r) & p(i_f, i_r) \leq 0 \\ \mod\ (p(i_f, i_r), z_f) & p(i_f, i_r) > 0 \end{cases} \tag{A.7}$$

where $\lfloor \cdot \rfloor$ is floor function and $\mod(\cdot)$ is the modulo function.

Following figures show the base matrices of WiMAX LDPC Codes that are used in this thesis work for the given code rates. The numbers in the matrices indicate the shift values $p(f, i_f, i_r)$. The value -1 indicates zero matrix and the value 0 indicates identity matrix.

$$\begin{bmatrix}
3 & 0 & -1 & -1 & 2 & 0 & -1 & 3 & 7 & -1 & 1 & 1 & -1 & -1 & -1 & -1 & 1 & 0 & -1 & -1 & -1 & -1 & -1 & -1 \\
-1 & -1 & 1 & -1 & 36 & -1 & -1 & 34 & 10 & -1 & -1 & 18 & 2 & -1 & 3 & 0 & -1 & 0 & 0 & -1 & -1 & -1 & -1 & -1 \\
-1 & -1 & 12 & 2 & -1 & 15 & -1 & 40 & -1 & 3 & -1 & 15 & -1 & 2 & 13 & -1 & -1 & -1 & 0 & 0 & -1 & -1 & -1 & -1 \\
-1 & -1 & 19 & 24 & -1 & 3 & 0 & -1 & 6 & -1 & 17 & -1 & -1 & -1 & 8 & 39 & -1 & -1 & -1 & 0 & 0 & -1 & -1 & -1 \\
20 & -1 & 6 & -1 & -1 & 10 & 29 & -1 & -1 & 28 & -1 & 14 & -1 & 38 & -1 & -1 & 0 & -1 & -1 & -1 & 0 & 0 & -1 & -1 \\
-1 & -1 & 10 & -1 & 28 & 20 & -1 & -1 & 8 & -1 & 36 & -1 & 9 & -1 & 21 & 45 & -1 & -1 & -1 & -1 & -1 & 0 & 0 & -1 \\
35 & 25 & -1 & 37 & -1 & 21 & -1 & -1 & 5 & -1 & -1 & 0 & -1 & 4 & 20 & -1 & -1 & -1 & -1 & -1 & -1 & -1 & 0 & 0 \\
-1 & 6 & 6 & -1 & -1 & -1 & 4 & -1 & 14 & 30 & -1 & 3 & 36 & -1 & 14 & -1 & 1 & -1 & -1 & -1 & -1 & -1 & -1 & 0
\end{bmatrix}$$

Figure A.1: WiMAX $R = 2/3$ A base matrix

$$\begin{bmatrix}
6 & 38 & 3 & 93 & -1 & -1 & -1 & 30 & 70 & -1 & 86 & -1 & 37 & 38 & 4 & 11 & -1 & 46 & 48 & 0 & -1 & -1 & -1 & -1 \\
62 & 94 & 19 & 84 & -1 & 92 & 78 & -1 & 15 & -1 & -1 & 92 & -1 & 45 & 24 & 32 & 30 & -1 & -1 & 0 & 0 & -1 & -1 & -1 \\
71 & -1 & 55 & -1 & 12 & 66 & 45 & 79 & -1 & 78 & -1 & -1 & 10 & -1 & 22 & 55 & 70 & 82 & -1 & -1 & 0 & 0 & -1 & -1 \\
38 & 61 & -1 & 66 & 9 & 73 & 47 & 64 & -1 & 39 & 61 & 43 & -1 & -1 & -1 & -1 & 95 & 32 & 0 & -1 & -1 & 0 & 0 & -1 \\
-1 & -1 & -1 & -1 & 32 & 52 & 55 & 80 & 95 & 22 & 6 & 51 & 24 & 90 & 44 & 20 & -1 & -1 & -1 & -1 & -1 & -1 & 0 & 0 \\
-1 & 63 & 31 & 88 & 20 & -1 & -1 & -1 & 6 & 40 & 56 & 16 & 71 & 53 & -1 & -1 & 27 & 26 & 48 & -1 & -1 & -1 & -1 & 0
\end{bmatrix}$$

Figure A.2: WiMAX $R = 3/4$ A base matrix

$$\begin{bmatrix}
1 & 25 & 55 & -1 & 47 & 4 & -1 & 91 & 84 & 8 & 86 & 52 & 82 & 33 & 5 & 0 & 36 & 20 & 4 & 77 & 80 & 0 & -1 & -1 \\
-1 & 6 & -1 & 36 & 40 & 47 & 12 & 79 & 47 & -1 & 41 & 21 & 12 & 71 & 14 & 72 & 0 & 44 & 49 & 0 & 0 & 0 & 0 & -1 \\
51 & 81 & 83 & 4 & 67 & -1 & 21 & -1 & 31 & 24 & 91 & 61 & 81 & 9 & 86 & 78 & 60 & 88 & 67 & 15 & -1 & -1 & 0 & 0 \\
68 & -1 & 50 & 15 & -1 & 36 & 13 & 10 & 11 & 20 & 53 & 90 & 29 & 92 & 57 & 30 & 84 & 92 & 11 & 66 & 80 & -1 & -1 & 0
\end{bmatrix}$$

Figure A.3: WiMAX $R = 5/6$ base matrix